Applied Mechanics and Materials Vol 679 (2014) pp 241-246
© (2014) Trans Tech Publications, Switzerland
doi:10.4028/www.scientific.net/AMM.679.241

Submitted: 2014-08-13
Accepted: 2014-08-13
Online: 2014-10-08

Comparison Induced Voltage Between 0.35 mm and 0.50 mm thicknesses 3% SiFe (NG) with Different Frequency

Dina Maizana[a], Y. Yanawati[b], and A. Nazifah[c]

Department of Electrical System Engineering, Universiti Malaysia Perlis, Malaysia

Email: [a]dina@unimap.edu.my, [b]yanawatiyahya@yahoo.com, and [c]nazifah45@gmail.com

Keywords –3% SiFe (NG), Single Sheet Tester (SST), Harmonic factor

Abstract – This paper presents the comparison induced voltage between 0.35 mm and 0.50 mm thicknesses 3% SiFe (NG) with different frequency which are 45 Hz, 50 Hz and 60 Hz by using Single Sheet Tester (SST). This experiment used to measure the search coil voltage L1N1 and L2N2 at two positions (1st position and 2nd position) and harmonic content. The analysis shows, at different frequency for both thicknesses, the value of search coil voltage L1N1 is higher than the search coil voltage L2N2 for both positions. It shows the easy direction is single sheet tester direction at the 1st position for 0.35 mm and 0.50 mm thickness with different frequency. For harmonic content, at 0.6 T with different frequency for both thicknesses, the 3rd order harmonic factor of 0.35 mm is lower than 0.50 mm thickness 3% SiFe (NG). It is because the higher losses can increase the harmonic of the materials. It means that harmonic is affected by ingredient and thicknesses in core material.

Introduction

There are two main kinds of electrical steel fully processed grain used in transformer and non grain used in induction motor. The fundamental difference among the both types is the magnetization direction in which the grain grades shows that the optimum magnetic behavior in one direction only, while the magnetic properties of grade non-grain is isotropic behavior. This is in accordance with the requirements of the standard application of these products are for the grain transformer and non grain to the motor / generator. Normal field lines need to explain why this machine rotating multidirectional magnetization, whereas for magnetization of the transformer in the body only requires the selection of the magnetization [1].

Therefore, grain and non-grain have different production process of thermo-mechanics, who take on the characteristics distinct magnetization, resulting is basically from crystallo graphic texture is different. This provides the magnetic properties of Grain towards improved rolling, while steel is not likely oriented features better in the transverse direction. Figure 3.3 shows the loss curve for M6 Grain grades from grade M235-35A is Non Grain. Grain steel output process, with a special texture Goss, is more complex than the Non Grain with a strong fiber texture, and this is reflected in higher prices of grain grade. Non grain has magnetic properties that are isotropic as possible. These material is manufactured multidirectional magnetization is useful for rotating machines [1].

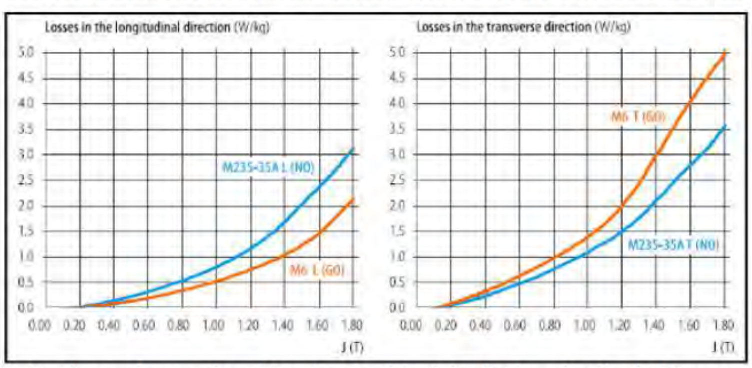

Figure 1: Grain has lower losses than Non-Grain (blue) in the longitudinal (L) sense, but higher in the transverse direction (T)

The significant improvement the magnetic efficiency can be identified by lamination. The eddy current and hysteresis losses can decrease by proper laminated magnetic materials. It also functions to radically decrease all the power dissipation in the core. The properties of materials where the material is made, specified and used on the pattern properties and applications such as Composition (a higher silicon which restrains eddy currents reduces loss, is harder and costs more to make and Silicon is added can range from zero up to 3+ %) and Thickness (The thinner of lamination the more effectively eddy currents are restrained and the lower the core losses) [2].

All metals and many non-metals have some sort of response to magnetic fields, and this response is measured by a number of magnetic properties. Figure 2 (a) and (b) shows the magnetic hysteresis curves. Based on Figure 2 (a) and (b), one of common way to rate a material's response to a magnetic field is by measuring the flux density (*B*) in the material when it is placed in a magnetic field of varying magnetic strength (*H*), and this field strength is increased and decreased. The slope of the *B-H* curve is a measure of the magnetic characteristics of a material, and the shape of the curve that results when the material is tested in a cyclic magnetic field is a measure of how the material will behave under such condition [3].

If a material magnetizes and demagnetizes easily, the *B-H* curve exhibits a hysteresis loop like that illustrated as shown in Figure 2 (a). A material that tends to remain magnetized as the field strength is decreased will have hysteresis loop resembling that illustrated as shown in Figure 2 (b). Low-carbon steels with from 0.5% to 5% silicon have a small hysteresis loop, and they are widely used for lamination in electric motors. The hard magnetic materials can make a good permanent magnet [3].

In this paper, the comparison on induced voltage between 0.35 mm and 0.50 mm thicknesses 3% SiFe (NG) with different frequency is presented.

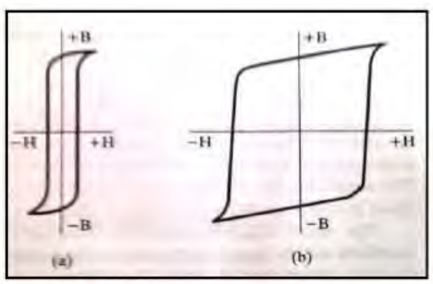

Figure 2: Magnetic Hysteresis Curves. (a) A soft magnetic material (easily magnetized and demagnetized material). (b) A hard magnetic material, one that retrains magnetism as in a permanent magnet.

Experimental Setup

Single Sheet Tester (SST) is the method used to find and measure induced voltage and nominal loss in the material on easy (rolling) and hard direction. Figure 3 shows the experimental setup for Single Sheet Tester (SST). Based on Figure 3, single sheet tester having closed magnetic path has a problem that measurement accuracy of magnetostriction is considerably affected by electromagnetic force between specimen and yoke. Therefore, an open type has been developed. The uniform flux distribution has been taken in sufficiently large region, installing a compensating magnetizing winding, and a method of waveform control was investigated.

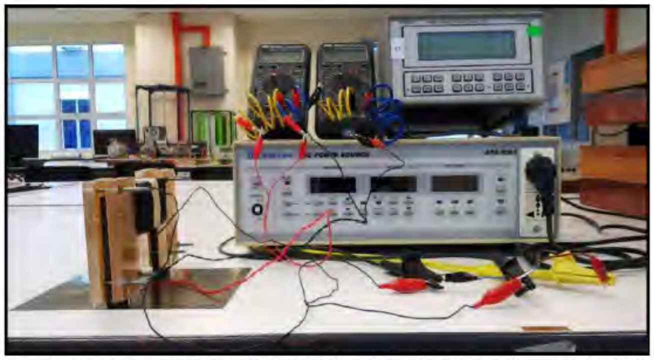

Figure 3: Experimental Setup for Single Sheet Tester (SST)

Figure 4 shows the block diagram for Single Sheet Tester (SST) with Single yoke. Based on Figure 4, this device operates on material properties with size enough to make effects due to cut edges insignificant. Flux closure yoke are used can be single or double sided. If single sided yoke, eddy current pools can form in the strip where flux leaves or enters its normal to its surface. With double sided yokes these eddy current effects largely cancel.

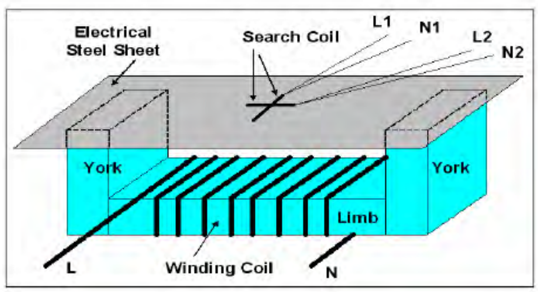

Figure 4: The Single Sheet Tester with Single Yoke

Input voltage was used to supply the voltage at winding coil with Tesla of flux density. Equation 1 was used to get the value of input voltage as shown below:

$$V = 4.44 \times B \times N \times f \times A \quad (1)$$

Where;

V	Voltage
4.44	Constant Value
B	Tesla
N	Number of winding turn = 125 turns
F	Frequency = 50 Hz
A	Cross sectional on the surface of yoke = $n \times t \times w$ $[m^2]$

- n Number of layer of yoke lamination = 40 layers
- t Thickness of yoke lamination [m] = 0.3 mm
- w Width of yoke lamination [m] = 3 cm

Result And Discussion

From experiment, the result shows that the voltage, current and power loss at the single sheet tester will be increase when the flux density increase for two position (1st position and 2nd position), but the voltage at the search coil at two position is different. Figure 5 shows the search coil voltage (L1N1 & L2N2) at two positions vs. flux density for both thicknesses at 50 Hz.

Based on the Figure 5, at 50 Hz for 0.35 mm and 0.50 mm thickness, it shows that the value of search coil voltage L1N1 is higher than the search coil voltage L2N2 for both positions which are 1st position and 2nd position. From the observation, it shows the easy direction is single sheet tester direction at the 1st position for 0.35 mm and 0.50 mm thickness.

Figure 6 (a) and (b) shows the search coil voltage (L1N1 & L2N2) at two positions vs. flux density (0.6 T) for 0.35mm and 0.50 mm thicknesses at different frequency which is 45 Hz, 50 Hz and 60 Hz. Based on the Figure 6 (a) and (b), at different frequency which is 45 Hz, 50 Hz and 60 Hz for 0.35 mm and 0.50 mm thickness, it shows that the value of search coil voltage L1N1 is higher than the search coil voltage L2N2 for both positions which are 1st position and 2nd position. From the observation, it shows the easy direction is single sheet tester direction at the 1st position for 0.35 mm and 0.50 mm thickness with different frequency.

Figure 7 shows the graph of 3rd order Harmonic Factor vs. Flux Density for 0.35 mm and 0.50 mm at 50 Hz. Based on Figure 7 at 50 Hz, refer to the all range of flux density from 0.2 T until 0.8 T, the 3rd order harmonic factor of 0.35 mm is lower than 0.50 mm thickness 3% SiFe (NG). At 0.6 T, the value of 3rd order harmonic factor of 0.35 mm is lower than 0.50 mm thicknesses which are 8.83% and 13.63% each. The 0.35 mm has lower of 35.22% for the 3rd order harmonic factor as compared to 0.50 mm thicknesses 3% SiFe (NG). It is because the higher losses can increase the harmonic of the materials.

Figure 8 shows the graph of 3rd order Harmonic Factor vs. Flux Density (0.6 T) for 0.35 mm and 0.50 mm thicknesses at different frequency which is 45 Hz, 50 Hz and 60 Hz. Based on the Figure 8, at 0.6 T with different frequency which is 45 Hz, 50 Hz and 60 Hz for 0.35 mm and 0.50 mm thickness, the 3rd order harmonic factor of 0.35 mm is lower than 0.50 mm thickness 3% SiFe (NG). At 45 Hz, the value of 3rd order harmonic factor of 0.35 mm is lower than 0.50 mm thicknesses which are 8.39% and 12.96% each. The 0.35 mm has lower of 35.26% for the 3rd order harmonic factor as compared to 0.50 mm thicknesses 3% SiFe (NG). At 50 Hz, the value of 3rd order harmonic factor of 0.35 mm is lower than 0.50 mm thicknesses which are 8.83% and 13.63% each. The 0.35 mm has lower of 35.22% for the 3rd order harmonic factor as compared to 0.50 mm thicknesses 3% SiFe (NG). At 60 Hz, the value of 3rd order harmonic factor of 0.35 mm is lower than 0.50 mm thicknesses which are 10.41% and 15.57% each. The 0.35 mm has lower of 33.14% for the 3rd order harmonic factor as compared to 0.50 mm thicknesses 3% SiFe (NG). It is because the higher losses can increase the harmonic of the materials.

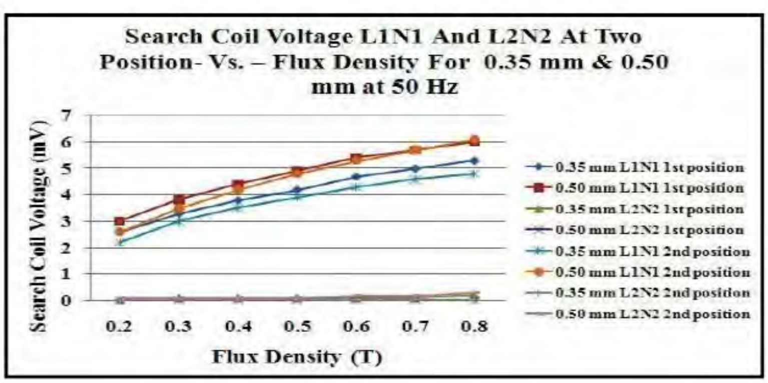

Figure 5: Search Coil Voltage (L1N1 & L2N2) at Two position vs. Flux Density for Both Thicknesses at 50 Hz

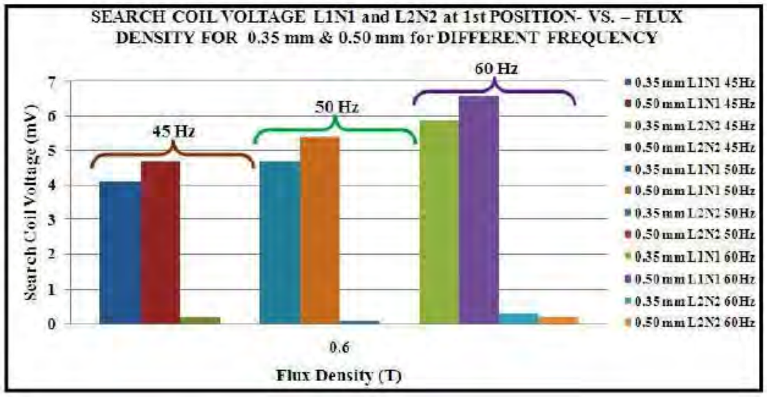

(a) 1st Position

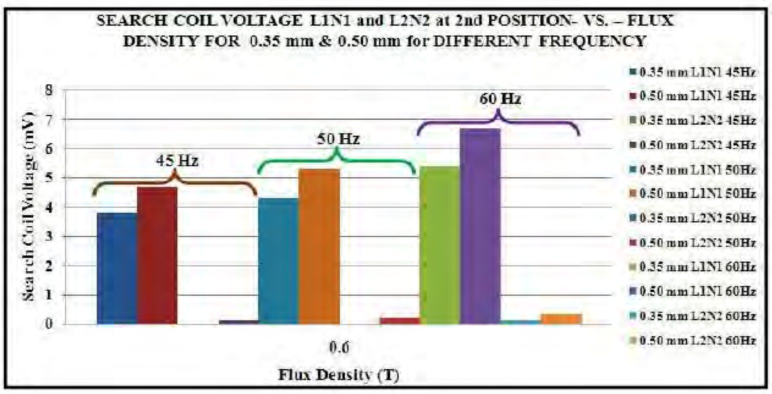

(b) 2nd Position

Figure 6: Search Coil Voltage (L1N1 & L2N2) at Two position vs. Flux Density (0.6T) for Both Thicknesses at Different Frequency

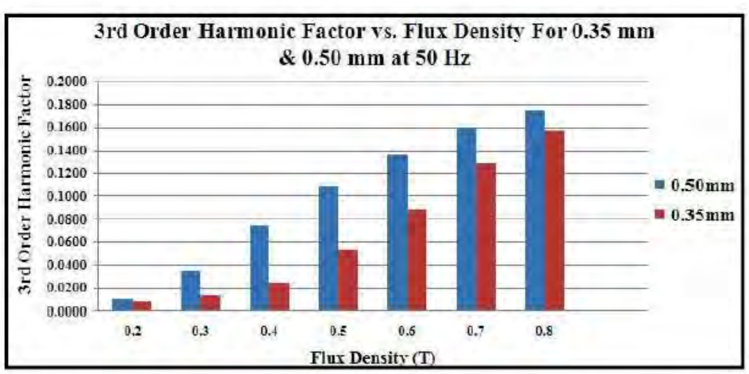

Figure 7: Graph of 3rd order Harmonic Factor vs. Flux Density for 0.35 mm and 0.50 mm thickness at 50Hz

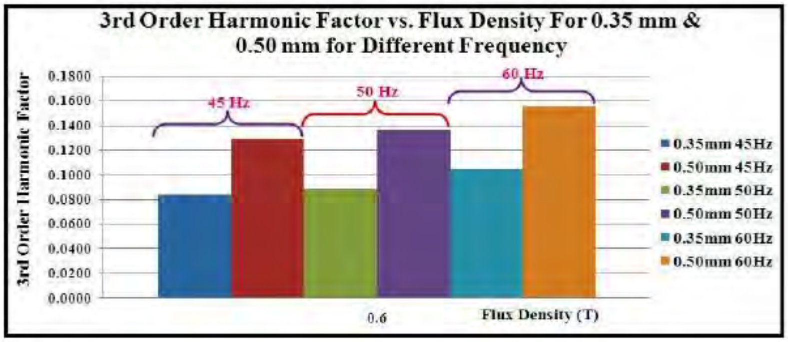

Figure 8: Graph of 3rd order Harmonic Factor vs. Flux Density (0.6T) for 0.35 mm and 0.50 mm thickness at Different Frequency

Conclusion

From the analysis, it shows that the search coil voltage (L1N1 & L2N2) at two positions for 0.35mm and 0.50 mm thicknesses at different frequency which is 45 Hz, 50 Hz and 60 Hz, the value of search coil voltage L1N1 is higher than the search coil voltage L2N2 for both positions which are 1st position and 2nd position. From the observation, it shows the easy direction is single sheet tester direction at the 1st position for 0.35 mm and 0.50 mm thickness with different frequency. For harmonic content is an important factor that influence on induction motor losses. At 0.6 T with different frequency which is 45 Hz, 50 Hz and 60 Hz for 0.35 mm and 0.50 mm thickness, the 3rd order harmonic factor of 0.35 mm is lower than 0.50 mm thickness 3% SiFe (NG). At 45 Hz, the 0.35 mm has lower of 35.26% for the 3rd order harmonic factor as compared to 0.50 mm thicknesses 3% SiFe (NG). At 50 Hz, the 0.35 mm has lower of 35.22% for the 3rd order harmonic factor as compared to 0.50 mm thicknesses 3% SiFe (NG). At 60 Hz, the 0.35 mm has lower of 33.14% for the 3rd order harmonic factor as compared to 0.50 mm thicknesses 3% SiFe (NG). It is because the higher losses can increase the harmonic of the materials. It does mean the harmonic effect caused by different induced voltage and different thickness of material.

Acknowledgment

This work is financially supported by Grant RAGS FASA 1/2012 (9018-00022).

References

[1] Europe, F. C. (06/2010). Non-oriented fully processed electrical steels

[2] Beckley P. (2002). Electrical Steels for rotating machines: IEE power and energy series; no.23.

[3] Kenneth G. Budinski & Michael K. Budinski (1999), "Engineering Materials Properties and Selection" Prentice Hall International, inc. six edition.

Engineering and Technology Research

10.4028/www.scientific.net/AMM.679

Comparison Induced Voltage between 0.35 mm and 0.50 mm Thicknesses 3% SiFe (NG) with Different Frequency

10.4028/www.scientific.net/AMM.679.241

2. https://www.scientific.net/AMM.679.112

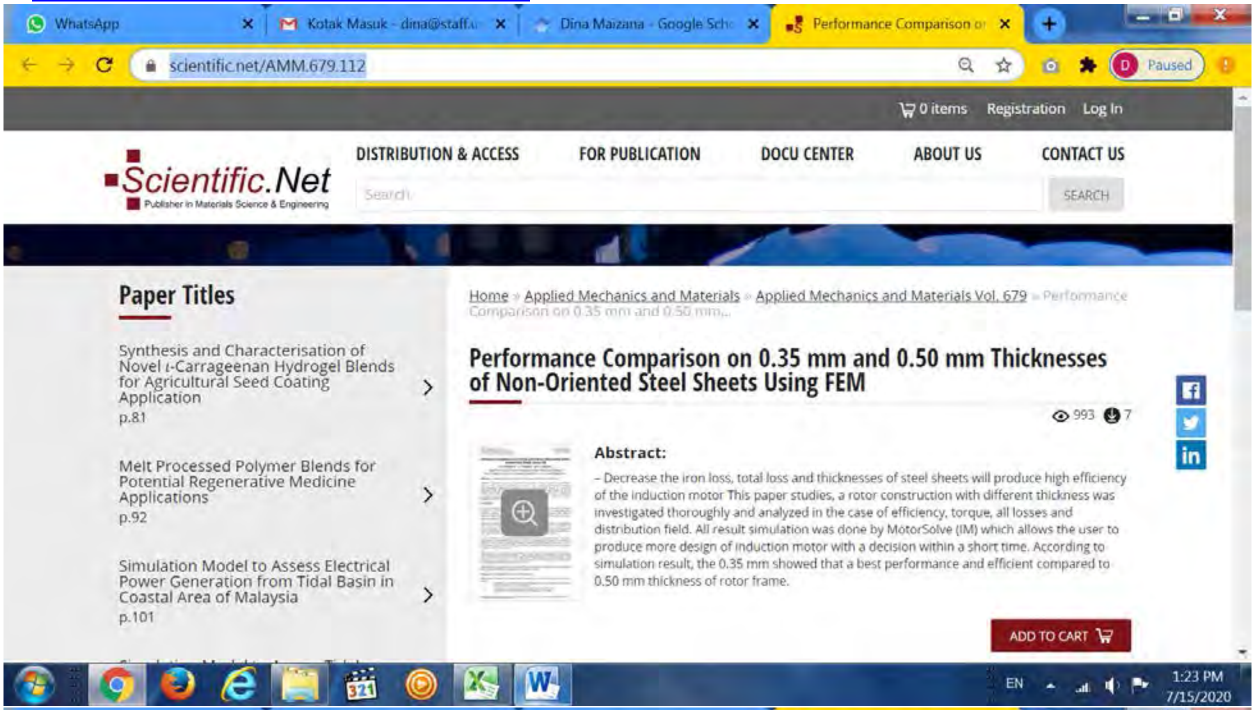

WhatsApp | Kotak Masuk - dina@staff.u | Dina Maizana - Google Sch | Performance Comparison o

scientific.net/AMM.679.112

0 items Registration Log In

Scientific.Net
Publisher in Materials Science & Engineering

DISTRIBUTION & ACCESS FOR PUBLICATION DOCU CENTER ABOUT US CONTACT US

Search SEARCH

Paper Titles

Synthesis and Characterisation of Novel ι-Carrageenan Hydrogel Blends for Agricultural Seed Coating Application
p.81

Melt Processed Polymer Blends for Potential Regenerative Medicine Applications
p.92

Simulation Model to Assess Electrical Power Generation from Tidal Basin in Coastal Area of Malaysia
p.101

Home » Applied Mechanics and Materials » Applied Mechanics and Materials Vol. 679 » Performance Comparison on 0.35 mm and 0.50 mm...

Performance Comparison on 0.35 mm and 0.50 mm Thicknesses of Non-Oriented Steel Sheets Using FEM

993 7

Abstract:

– Decrease the iron loss, total loss and thicknesses of steel sheets will produce high efficiency of the induction motor This paper studies, a rotor construction with different thickness was investigated thoroughly and analyzed in the case of efficiency, torque, all losses and distribution field. All result simulation was done by MotorSolve (IM) which allows the user to produce more design of induction motor with a decision within a short time. According to simulation result, the 0.35 mm showed that a best performance and efficient compared to 0.50 mm thickness of rotor frame.

ADD TO CART

EN 1:23 PM 7/15/2020

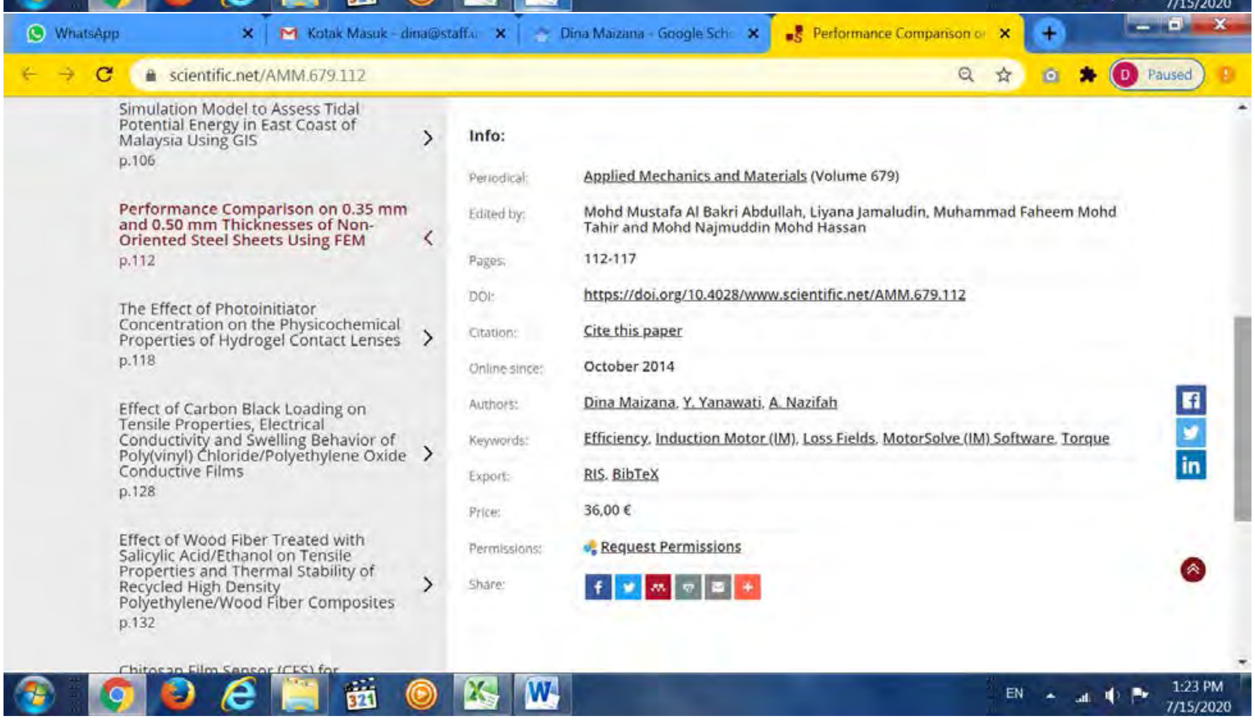

WhatsApp | Kotak Masuk - dina@staff.u | Dina Maizana - Google Sch | Performance Comparison o

scientific.net/AMM.679.112

Simulation Model to Assess Tidal Potential Energy in East Coast of Malaysia Using GIS
p.106

Performance Comparison on 0.35 mm and 0.50 mm Thicknesses of Non-Oriented Steel Sheets Using FEM
p.112

The Effect of Photoinitiator Concentration on the Physicochemical Properties of Hydrogel Contact Lenses
p.118

Effect of Carbon Black Loading on Tensile Properties, Electrical Conductivity and Swelling Behavior of Poly(vinyl) Chloride/Polyethylene Oxide Conductive Films
p.128

Effect of Wood Fiber Treated with Salicylic Acid/Ethanol on Tensile Properties and Thermal Stability of Recycled High Density Polyethylene/Wood Fiber Composites
p.132

Chitosan Film Sensor (CFS) for

Info:

Periodical:	Applied Mechanics and Materials (Volume 679)
Edited by:	Mohd Mustafa Al Bakri Abdullah, Liyana Jamaludin, Muhammad Faheem Mohd Tahir and Mohd Najmuddin Mohd Hassan
Pages:	112-117
DOI:	https://doi.org/10.4028/www.scientific.net/AMM.679.112
Citation:	Cite this paper
Online since:	October 2014
Authors:	Dina Maizana, Y. Yanawati, A. Nazifah
Keywords:	Efficiency, Induction Motor (IM), Loss Fields, MotorSolve (IM) Software, Torque
Export:	RIS, BibTeX
Price:	36,00 €
Permissions:	Request Permissions
Share:	

EN 1:23 PM 7/15/2020

Applied Mechanics and Materials Vol. 679 (2014) pp 112-117
© (2014) Trans Tech Publications, Switzerland
doi:10.4028/www.scientific.net/AMM.679.112

Submitted: 2014-08-12
Accepted: 2014-08-13
Online: 2014-10-08

Performance Comparison on 0.35 mm and 0.50 mm thicknesses of Non-oriented Steel Sheets Using FEM

Dina Maizana[a], Y. Yanawati[b], and A. Nazifah[c]

Department of Electrical System Engineering Universiti Malaysia Perlis, Malaysia

Email: [a]dina@unimap.edu.my, [b]yanawatiyahya@yahoo.com, and [c]nazifah45@gmail.com

Keywords – Efficiency, torque, loss fields, induction motor, MotorSolve (IM) Software

Abstract – Decrease the iron loss, total loss and thicknesses of steel sheets will produce high efficiency of the induction motor This paper studies, a rotor construction with different thickness was investigated thoroughly and analyzed in the case of efficiency, torque, all losses and distribution field. All result simulation was done by MotorSolve (IM) which allows the user to produce more design of induction motor with a decision within a short time. According to simulation result, the 0.35 mm showed that a best performance and efficient compared to 0.50 mm thickness of rotor frame.

Introduction

In 1888, the induction motor was invented by Nikola Tesla. Induction motors can be used effectively in all motor application, except where very high torque or very fine adjustable speed control is required. Induction machines represent a class of rotating apparatus that includes induction motors, induction generators, induction frequency converters, induction phase converters and electromagnetic slip couplings [1].

There are two types of rotor construction which are squirrel-cage and wound rotor. A squirrel-cage rotor consists of a set aluminium or copper bars was installed into the rotor bars slot which are all the rotor bars was connected to the end ring. Wound-rotor made up of three sets winding covered with the connection is carried out on three slip rings fitted to one end of the shaft. Wound-rotor are more expensive than squirrel-cage rotor and they require much more maintenance [2].

In 1997, manufacturer of motor would no longer be able to provide a standard-efficiency of motors. The solution for that problem, The Energy Act of 1992 was defines and produces a new efficiency levels for several electrical component including motors. They assumed that a motor worn out, the replacement of motor will be the bid high-efficiency. Assemble the efficienct of motors can reduce energy loss in induction motor [3].

Eddy currents are prevented by laminating. Skin would has emfs induced inside during magnetization reversal and arising residual of energy 'eddy currents' by dissipate heat. If the metal core are divided into thin slices residual eddy current path resistance and emf change due to the overall power dissipation in the core were radical decrease. The thin sheet steel was effective eddy current was prevented and decrease the core loss [4].

The performance comparison on 0.35 mm and 0.50 mm thicknesses of Non-oriented Electrical Steel Sheets for Induction Motor was presented in this paper reseaarch.

Designing The Modeling By MotorSolve (IM) Software

Methodology employed for the completion of these inquiries was divisible into three main sections, namely:

1. Designing a rotor frame with different thicknesses of non-oriented electrical steel sheets which are 0.35 mm and 0.50 mm
2. Simulation result on both thicknesses of steel sheet for rotor frame.
3. Analysis result on both thicknesses of steel sheet for rotor frame.

The induction motor with round rotor bar and parallel round stator was chosen for this simulation. Figure 1 shows the design with rotor bar and stator slot type. Based on Figure 1, the model of the induction motor is 3-phase, 0.5 Hp, 420 V, 50 Hz with 30 rotor bars of Round Bar rotor type and 24 stator slots of Parallel Round teeth. Only the thickness for rotor frame was changed for each simulation.

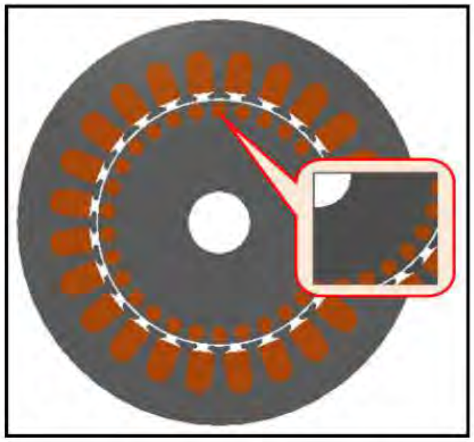

Figure 1: Round Bars Rotor Type and Parallel Round Stator Type

Based on Figure 1, it shows the round bar rotor slot type. The use of this slot design is since it has 'bar started' discretely separate of the main body of the conductor bar with the 'leak slot", connected to the motor by a high conductivity material in the rotor cage. In addition, this design has a rotor bar rotor torque locked and slip each is higher [5].

The result is then compiled to Table 1 which is the nameplate data of 0.5 Hp induction motor for 0.35 mm and 0.50 mm thickness non-oriented steel sheets. The input like motor horse power, input voltage and frequency are included in software simulation and the remaining result in Table 1 are output from the MotorSolve (IM) software simulation.

Table 1: 3-Phase 0.5Hp induction motor nameplates for both thicknesses

0.35 mm		0.5 mm	
Phase	3	**Phase**	3
Frequency	50	**Frequency**	50
Voltage	420	**Voltage**	420
RPM	1425	**RPM**	1425
Current	1.1746	**Current**	1.1988
Horsepower	0.5	**Horsepower**	0.5
Power Factor	0.6216	**Power Factor**	0. 6153
Efficiency	76.92	**Efficiency**	76.76

Analysis And Discussion

The design of induction motor was analyzed by using analysis and performance charts for the features such as efficiency, torque, iron loss, total loss, and eddy current loss.

Figure 2 shows the efficiency vs. Speed for both thicknesses which are 0.35 mm and 0.50 mm non-oriented electrical steel sheets for rotor frame. Based on Figure 2, the graph shows that the value of efficiency for 0.35 mm is higher than 0.50 mm thicknesses, which are76.92% and 76.77%

respectively. The 0.35mm has an increment of 0.2% for the efficiency as compared to 0.50 mm. It is because the lower losses can increase the efficiency of the induction motor.

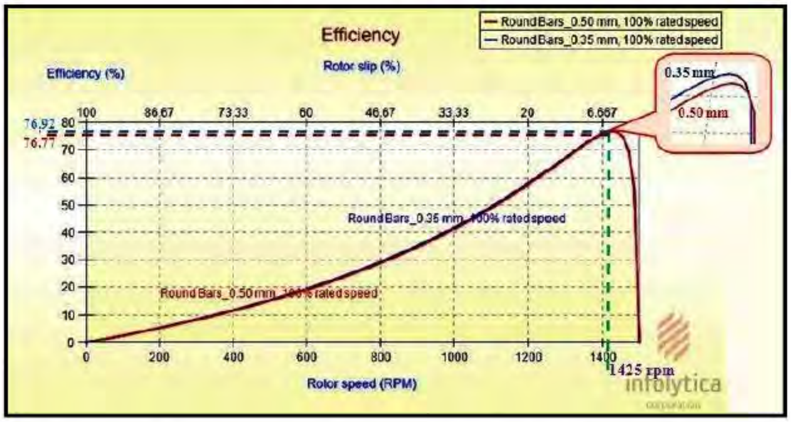

Figure 2: Graph Efficiency vs. Speed for both thicknesses of rotor frame

Figure 3 shows the torque vs. speed for both thicknesses of steel sheets. Refer to the simulation result, based on Figure 3, it showed that the 0.35 mm broken torque linear faster than the 0.50 mm thicknesses which are 7.61 Nm and 7.67 Nm each. It shows that 0.35mm is better than 0.50 mm thickness of material. This is because for the 0.35 mm, at a faster speed fractional, the heat produced from the motor is less, the terms of the rotor core is commonly associated with loss or core loss can be minimized and can even render damage to the motor at a minimum compared to 0.50 mm thickness.

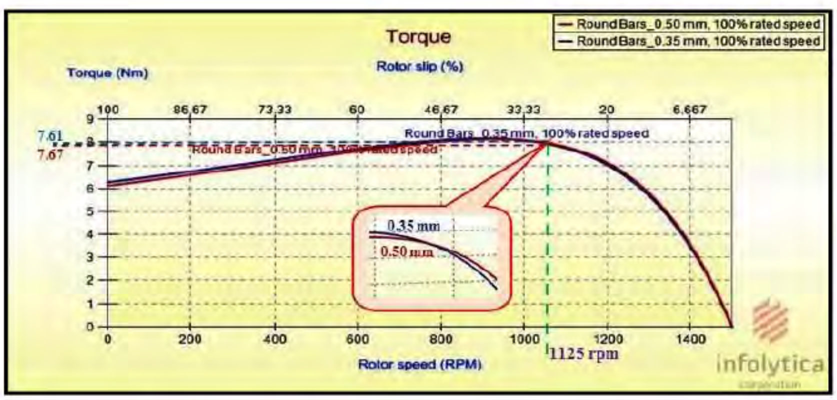

Figure 3: Torque vs. Speed for both thicknesses of Steel Sheet

Iron losses occur in all parts of the iron as the magnetic field of different machines. Iron loss has two components, hysteresis and eddy current losses that occur in other parts of iron depends on the frequency of the voltage are required. Figure 4 shows the graph of Iron Loss vs. Speed for both thicknesses of steel sheets. At 1425 rpm, the value of iron losses for 0.35 mm and 0.50 mm thickness are 4.05 Watt and 4.07 Watt. The 0.35 mm decreased of 0.5% for iron loss compared to the 0.50 mm thickness of steel sheet. It is because; decrement of lamination steel sheet can reduce the iron loss.

Figure 4: Iron Loss vs. Speed for both thicknesses of steel sheets

At 1425 rpm the total losses for 0.35 mm thickness are 121.35 Watt where else for 0.50 mm it is 125.94 Watt as shown as Figure 5. This shows that the power loss for 0.35 mm is lower than the 0.50 mm thickness of non-oriented electrical steel sheets.The 0.35 mm decreased of 3.64% for total loss compared to the 0.50 mm thicknesses of steel sheet. This is because 0.35 mm thickness has lower resistivity and lower the heat generated compared to the 0.50mm at that rpm.

Figure 5: Total Loss vs. Speed for both thicknesses of steel sheets

Figure 6 (a) and (b) shows the comparison of Hysteresis-Lamination Eddy Current Loss for 0.35 mm and 0.50 mm thickness non-oriented electrical steel.

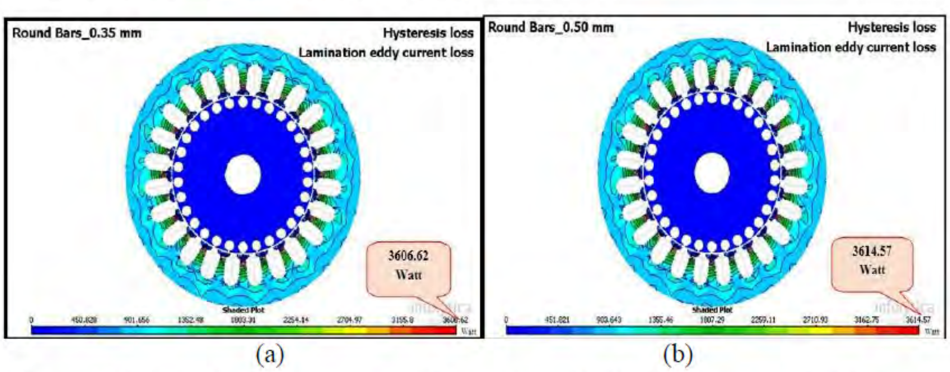

Figure 6: Hysteresis-Lamination Eddy Current Loss for Both Thicknesses Steel Sheets

Figure 6 (a) and (b) was shows the comparison between two different thicknesses in terms of eddy current loss. Both of the Figure shows that the lamination eddy current loss for 0.35 mm has lower than 0.50 mm thickness of rotor frame. The values of lamination eddy current loss for both thicknesses are 3606.62 Watt and 3614.57 Watt each. The 0.35 mm shows 0.23% lower lamination eddy current loss compared to 0.50 mm thickness. The lamination eddy current loss can reduces with decreasing thickness of rotor frame.

Based on Figure 7 (a) and (b), it shows the Current Density for 0.35 mm has higher than 0.50 mm thickness of rotor frame. The values of current density for both thicknesses are 2.90952 Ampere/mm^2 and 2.90792 Ampere/mm^2 each. The 0.35 mm shows 0.055% higher current density compared to 0.50 mm thickness. The total current is higher when the current flow into a smaller rotor bars. It can caused the amount of torque will be higher than the bigger rotor bars. The value of current and flux density will be change due to the rotor bars size, thinner and losses.

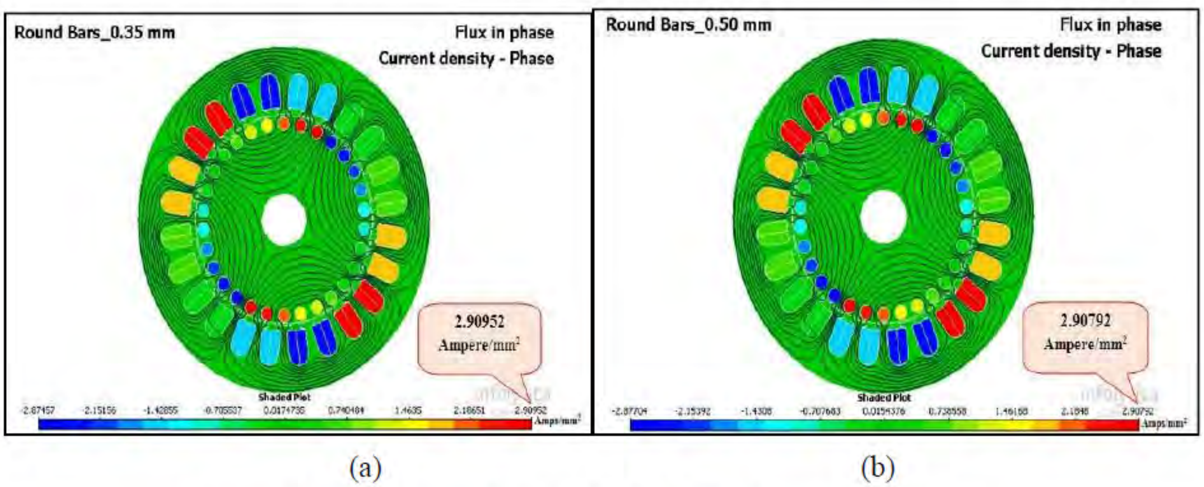

Figure 7: Flux-Current Density for Both Thicknesses Steel Sheets

Conclusion

Based on the simulation result, it shows that the 0.35 mm has an increment of 0.2% for the efficiency, broken torque linear faster, a decrement of 0.5% for iron loss,a decrement of 3.64% for total loss, a decrement of 0.23% lamination eddy current loss and increment of 0.055% for current density as compared to that of 0.50 mm thicknesses steel sheet. Increament of efficiency and power factor in induction motor can decrease harmonic and motor energy losses. Reduce the lamination of steel sheet can decrease the eddy current loss. The magnetic core loss can also be reduced by using thinner lamination in the magnetic structure.

Acknowledgment

This work is financially supported by Grant RAGS FASA 1/2012 (9018-00022).

References

[1] Chapman, S. J. (Ed.). (2005). Electric Machinery Fundamentals (fourth ed.): McGraw Hill.

[2] Bottauscio, O., Chiampi, M., Concari, C.,Tassoni, C., &Zucca, M. (2008). From the ideal to the real induction machine: Modelling approach and experimental validation. Journal of Magnetism and Magnetic Materials, 320(20), e901-e906.

[3] PT Design (1997). Motors, Power transmission design, vol. A340.

[4] Beckley P. (2002). Electrical Steels for rotating machines: IEE power and energy series; no.37.

[5] I. Daut, Y. Yanawati, N. Gomesh, S. Nor Shafiqin, M. Abdullah, I. Pungut (2010). "*Comparison of Torque between Different Diameters of Copper Rotor bar slot by Using FEM Software.*" 2010 3rd International Conference on Computer and Electrical Engineering (ICCEE 2010), 16-18 November 2010, Chengdu, China.

Engineering and Technology Research
10.4028/www.scientific.net/AMM.679

Performance Comparison on 0.35 mm and 0.50 mm Thicknesses of Non-Oriented Steel Sheets Using FEM
10.4028/www.scientific.net/AMM.679.112

3. https://www.scientific.net/AMM.679.261

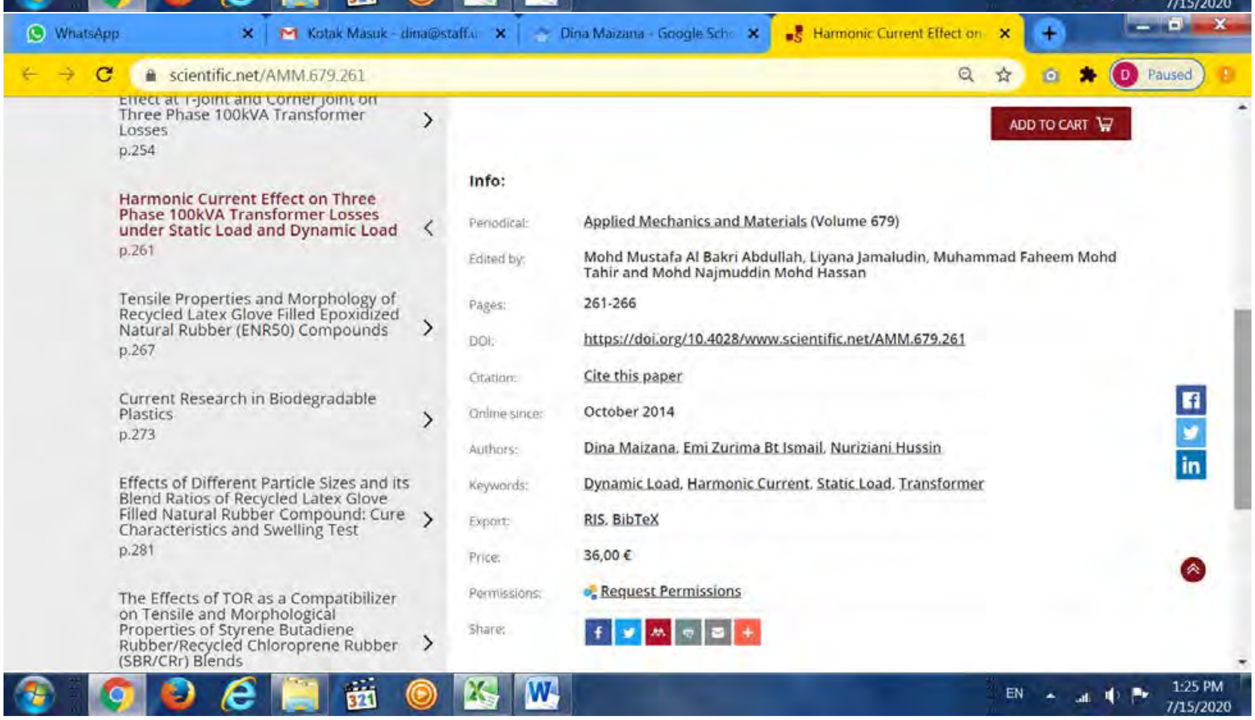

Applied Mechanics and Materials Vol. 679 (2014) pp 261-266
© (2014) Trans Tech Publications, Switzerland
doi:10.4028/www.scientific.net/AMM.679.261

Submitted: 2014-08-13
Accepted: 2014-08-13
Online: 2014-10-08

Harmonic Current Effect on Three Phase 100kVA Transformer Losses under Static Load and Dynamic Load

Dina Maizana [a] , Emi Zurima Bt Ismail [b], Nuriziani Hussin [c]

Department of Electrical System Engineering

Universiti Malaysia Perlis, Malaysia

E-mail: [a]dina@unimap.edu.my, [b]ezurima@gmail.com, [c]nuriziani@unimap.edu.my

Keywords: Harmonic current, static load, dynamic load, transformer

Abstract. This paper describes the harmonic current effect under static and dynamic load on 3 phase 100kVA transformer model. The methodology that used to measure a harmonic current is using power analyzer with different excitation. The experiment is conducted by changing input voltage with different flux density. A waveform can be obtained by using the data collected. 3rd order of harmonic gives a high impact to the complex waveform. At 0.6 Tesla, 50 Hz, the 3rd order of harmonic current under static load and dynamic load is 0.00196A and 0.26746A respectively. Therefore, both static and dynamic load were give an effect to harmonic current effect on transformer. This is because when the transformer connected to the load, more current and voltage induced in order to energize the load. Moreover, the loads itself have their own harmonic effect because of the functional mechanism.

Introduction

Distribution transformer is a transformer with a primary voltage of equal to or less than 35kV, a secondary voltage equal to or less than 600V, a frequency of 55-65Hz, a capacity of 10kVA to 2500kVA for liquid-immersed units and 15kVA to 2500kVA for dry-type units[1]. The performance of transformer will give a high impact to the whole power system. They are a lot of cases can be explored from transformer. In static load, force, pressure, gravity and applied gradually into an object [2]. Examples of static load are resistor, capacitor, LED and fluorescent lamp. Dynamic load is the presence of an outside force effecting an object or structure. The forces applied in dynamic load are usually unstable and constantly changing. Examples of dynamic load are induction motor and electric fan [7]. Harmonic is a distortion that can effect on transformer. The overall effect of harmonic is an increase in transformer heating [3].The value of the fundamental frequency or first order harmonic is 50 Hz. The second order of harmonics has a frequency of 100 Hz. The third order of harmonic has a frequency of 150 Hz. The fourth harmonic has a frequency of 200 Hz [4]. The transformer core design also give an effect to power losses. Different cutting angle such as 23°, 45 ° and 60° at the T-joint was introduced in order to find out the most efficient design. The localised flux density was measured using the search coil. The fundamental, third and fifth harmonic in the normal and in-plane flux density were measured at the corner joint and T-joint [5, 6].

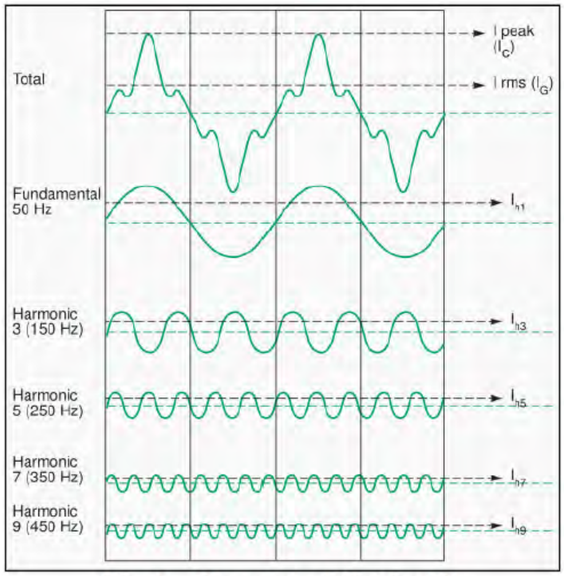

Fig. 1: Harmonic definition [4]

Fourier series can be used to show how a complex waveform is constructing. It is actually sum of all order of harmonic current occurred. The equation for harmonic content shows below:

$$Y = F_0 + F_1 \sin(\omega t + \varphi_1) + F_2 \sin(\omega t + \varphi_2) + \cdots + F_n \sin(\omega t + \varphi_n) \quad (1)$$

Hence, the reason of this investigation is to analyze the relationship between harmonic current effect and static load using 100kVA transformer model.

Experimental setup

The experiment was done by using three phase 1000kVA transformer. This transformer consists of 254 turns for both primary and secondary winding. 3% SiFe Cold Rolled Grain Oriented, (CRGO) M5 is used as core lamination and total number of layer is 35. The core thickness is 0.3mm and 10cm as width. The overlapping of core lamination is 0.5cm length.

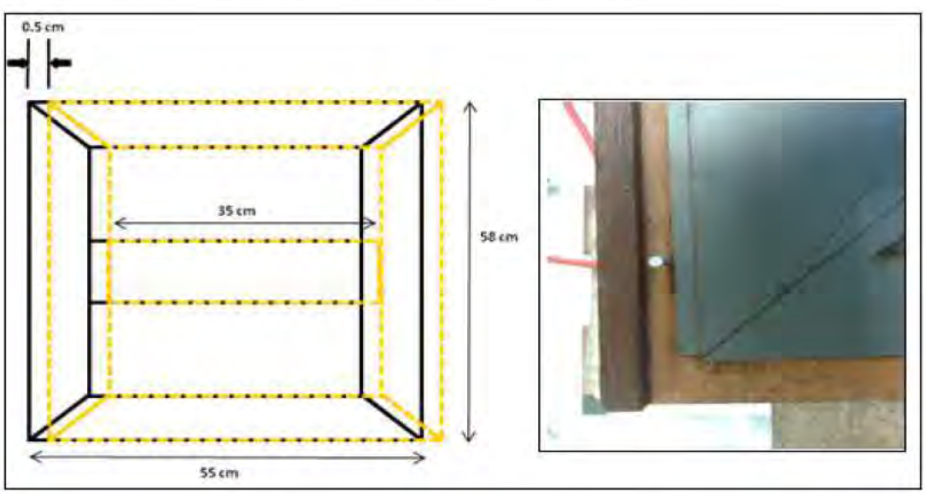

Fig. 2: Arrangement of the transformer core

The static load used in this investigation is incandescent lamp while for dynamic load used was three - phase machine board. The power for each incandescent lamp is 5W and delta connection used on both load in order to balance the voltage. The input voltage for three – phase machine board is 220V.

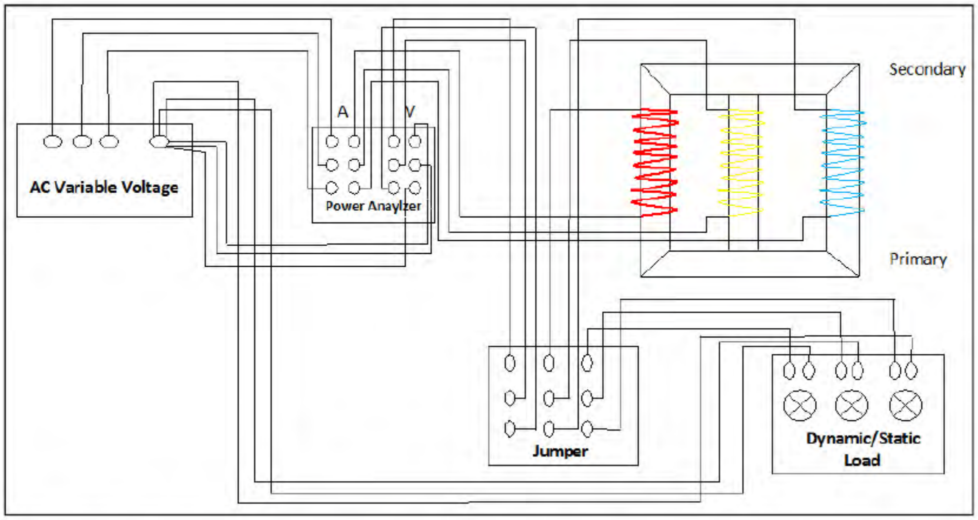

Fig. 3: The experiment setup for static and dynamic load (single line diagram)

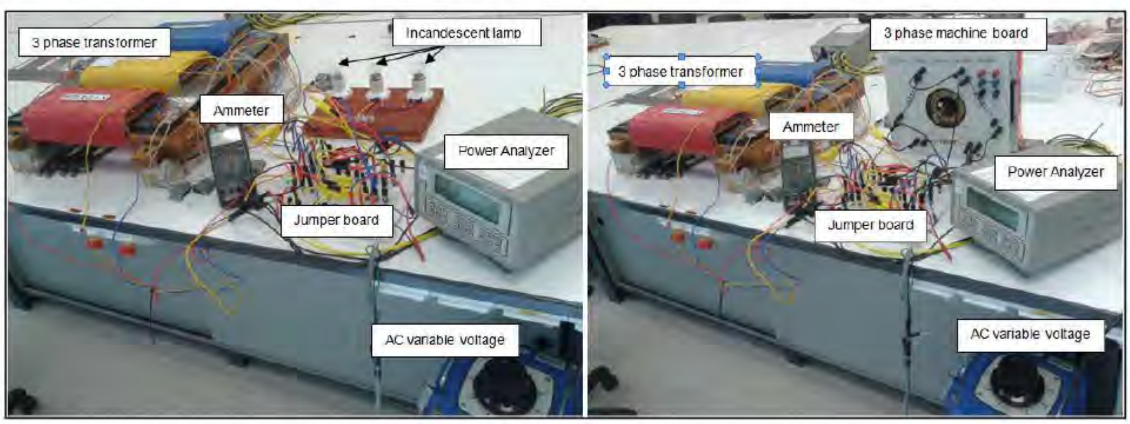

Fig. 4: The real experiment setup for static and dynamic load

For arrangement of the equipment, the power analyzer was connected to ac variable current and gave an input current. The secondary side of transformer gave voltage to power analyzer. The experiment was conducted by changing input voltage with different flux density. Fig. 3 shows the arrangement of the equipment. AC variable voltage as input was adjusted from 0.2T to 2.0T at 50 Hz. The equation used to get the input voltage is shows below:

$$V = 4.44 \times B \times N \times f \times A \quad (2)$$

Where:

V = Voltage, 4.44 = Constant, B = Flux density (Tesla), N = Number of winding turn = 254 turns, f = Frequency = 50 Hz

Table 1 shows the calculation result by using Equation 2 for input voltage from 0.2T until 2.0T at 50 Hz.

Table 1: Calculation result for input voltage

Flux density, B [Tesla]	Input Voltage, V_{in} [Volt]
0.2	11.97
0.4	23.93
0.6	35.90
0.8	47.86
1.0	59.83
1.2	71.80
1.4	83.76
1.6	95.73
1.8	107.70
2.0	119.66

Result & Discussion

After getting a data from the experiment, the value is transformed into a graph format using Matlab software. Fig. 3 and Fig. 4 show a waveform obtained from the experiment data by using static load and dynamic load respectively at 0.6 Tesla, 50 Hz. All of the harmonic waveforms are labelled for easy observation. The 3rd harmonic shows the highest compared to 4th, 5th, 6th and 7th harmonic for both loads.

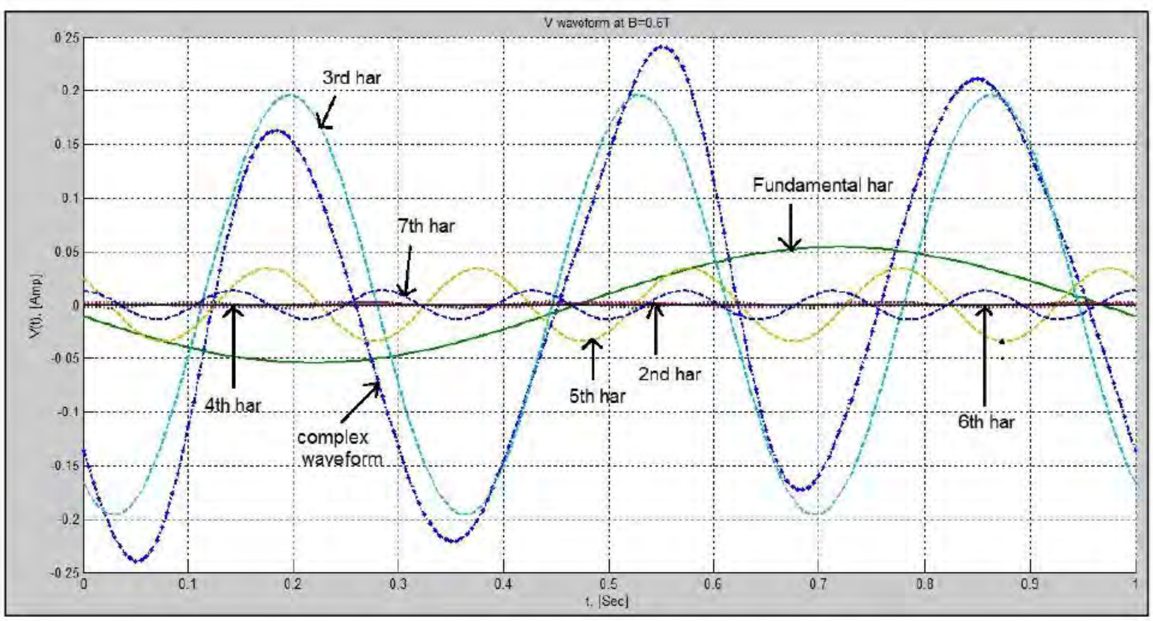

Fig. 3: A waveform for static load at B=0.6T, 50Hz

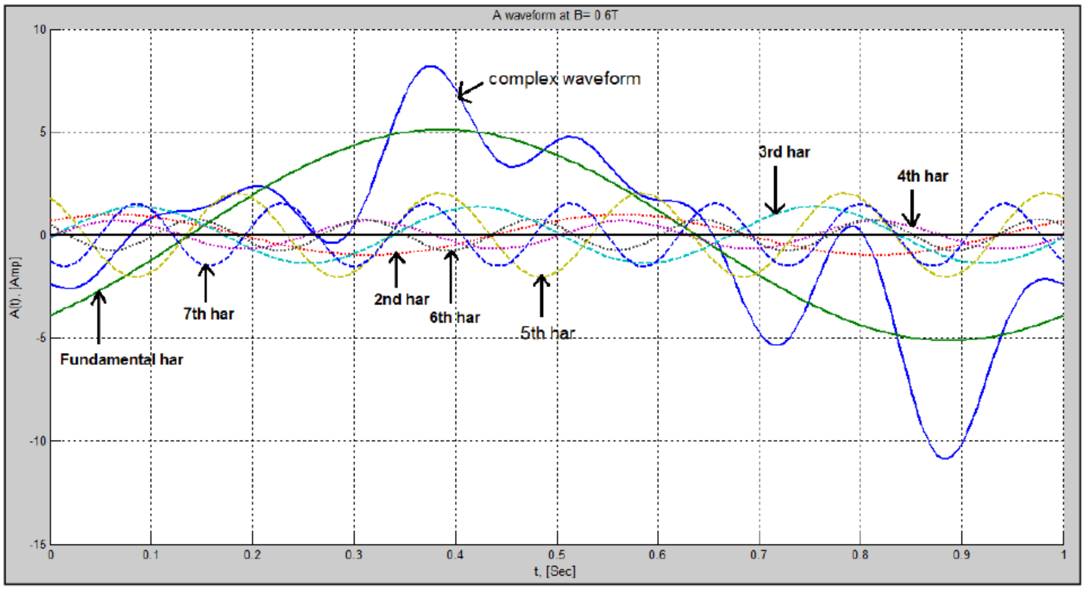

Fig. 4: A waveform for dynamic load at B=0.6T, 50Hz

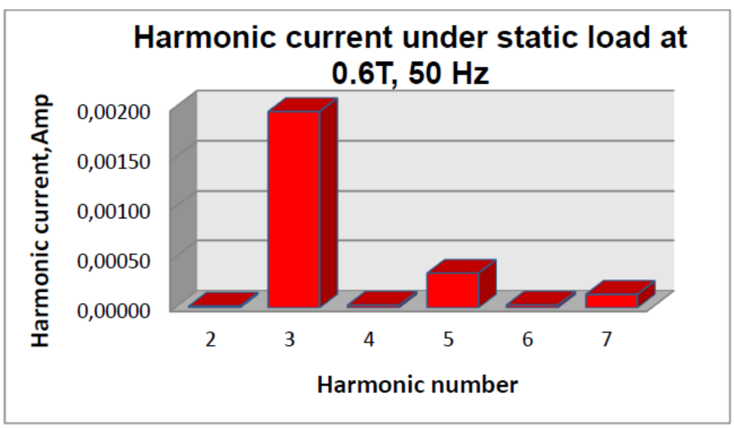

Fig. 5: Harmonic current under static load at 0.6T, 50 Hz

Fig. 5 and 6 shows the harmonic current for 2nd, 3rd, 4th, 5th, 6th and 7th order under static and dynamic load at 0.6Tesla, 50 Hz. From Fig.5, the highest harmonic was at 3rd order which is 0.00196A while the lowest was at 2nd order which is 0.00002A. For Fig.6, the highest harmonic was at 3rd order which is 0.26746A and the lowest was at 4th order which is 0.006724A. This is because when doing no load test, the secondary side of transformer was set to be open circuit. So, there is no current flow to the output terminal. Unfortunately, the small scale of harmonic current still exists in condition of flux transfer mechanism on core lamination. The flux only move around inside of the transformer core itself. When connected to the load, the load current should not be zero. This is because when load is connected, it needed more voltage in order for it to function. Hence, the voltage at secondary of transformer should be higher compared to voltage at primary. Flux inside the transformer core need to be transferred to the secondary output cable and to the load itself. Furthermore, the loads itself already contained harmonic because of their own functional mechanism.

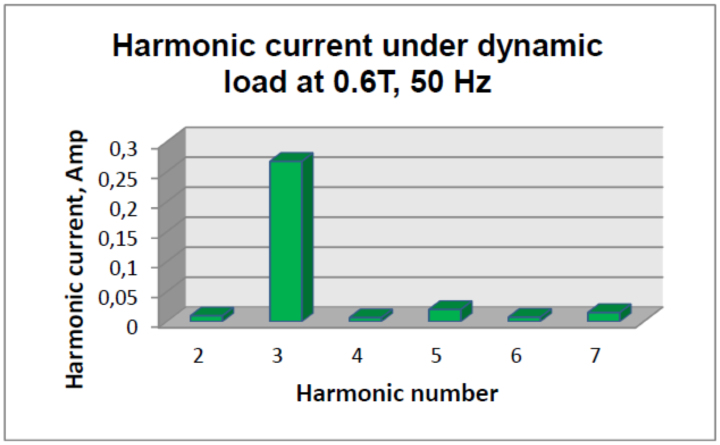

Figure 6: Harmonic current under dynamic load at 0.6T, 50 Hz

Summary

Static and dynamic load give an effect to harmonic current on 3 phase 100kVA transformer. Harmonic current under dynamic load is higher than under static load for about 99.27%. However, both loads still give an effect to harmonic current on transformer. This is because when the transformer connected to the loads, more current and voltage induced in order to energize the load. Flux inside the transformer core will be transferred to the secondary output cable and to the load itself.

Acknowledgement

This work is financially supported by Grant RAGS FASA 1/2012 (9018-00025).

References

[1] Test Procedures for Distribution Transformers, Building Technologies Program Office of Energy Efficiency and Renewable Energy U.S Department of Energy, lecture note.

[2] Information on Prof. Dr. Zahid A.Siddiqi , UET, Lahore, http://pec.org.pk/sCourse_files/CEC5-3.pdf, lecture note.

[3] Information on ecmweb.com/content/harmonic-distortion-definitions-and-countermeasures-part-2, updated on May 1 1998, obtained on March 2 2014.

[4] Information on http://electrical-engineering-portal.com/definition-of-harmonics-and-their-origin, last update on Sept 17 2012, obtained on June 13 2013.

[5] Shuhaimi, Zakaria@Abdullah, 'Flux density and power loss distribution in 100kVA Distribution Transformer core assembled with different cutting angle of T-joint', School of Electrical Systems Engineering (Thesis), UniMAP , 2010.

[6] Ismail Daut, Syafruddin Hasan, and Soib Taib, 'Magnetizing Current, Harmonic Content and Power Factor as the Indicators of Transformer Core Saturation', Journal of Clean Energy Technologies, Vol. 1, No. 4, October 2013.

[7] K. Y. Yoon and S. S. Rao, 'Dynamic Load Analysis of Spur Gears Using a New Tooth Profile', Journal of Mechanical Design, Volume 18, Issue 1, Pg 1-6,December 2007.

Engineering and Technology Research
10.4028/www.scientific.net/AMM.679

Harmonic Current Effect on Three Phase 100kVA Transformer Losses under Static Load and Dynamic Load
10.4028/www.scientific.net/AMM.679.261

4. https://www.scientific.net/AMM.679.254

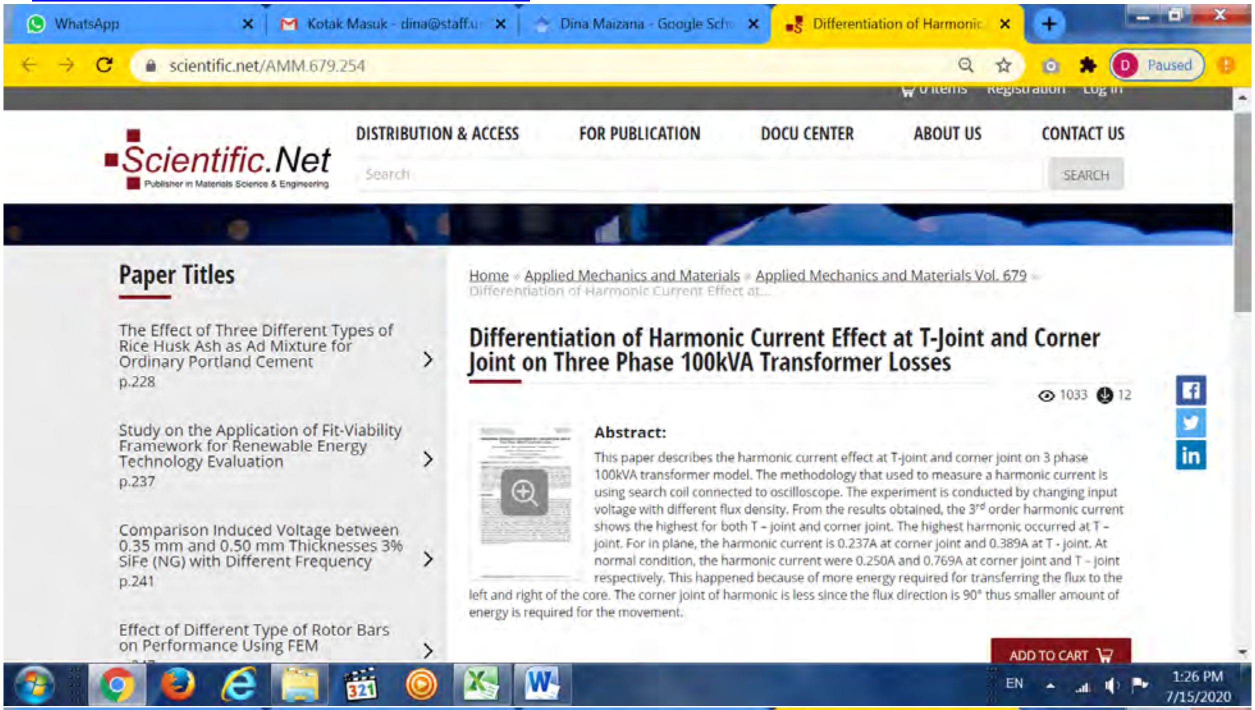

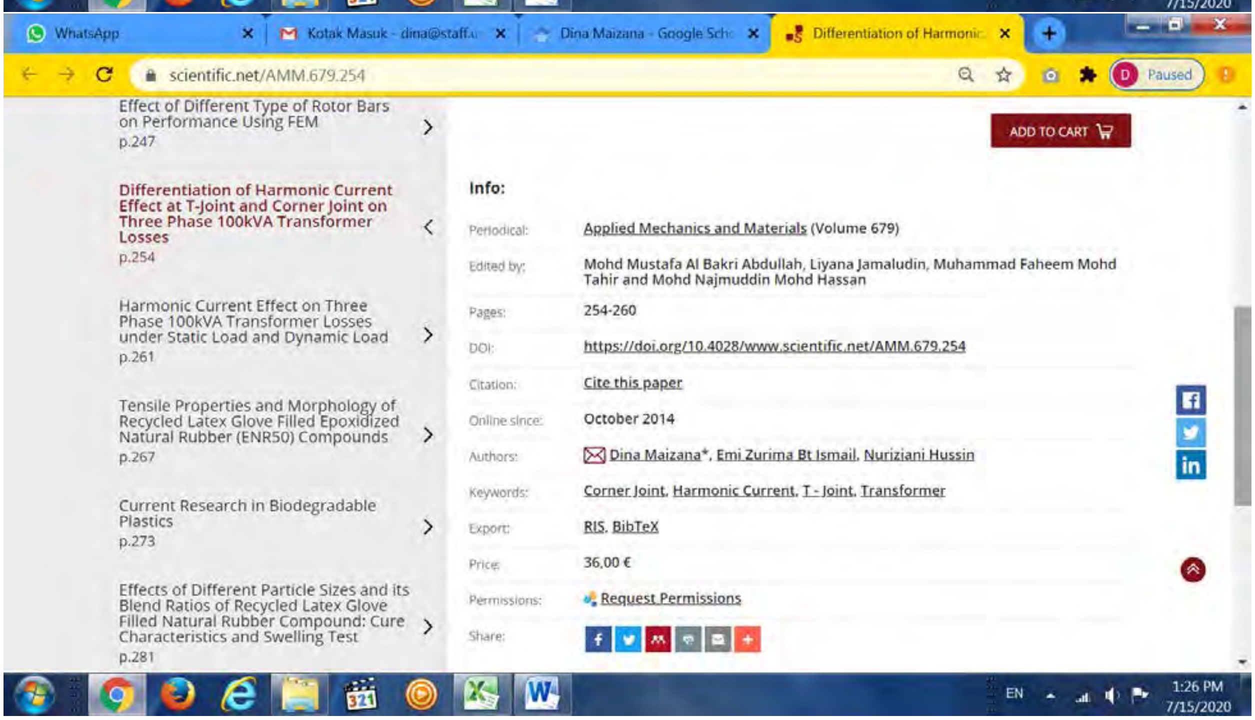

Applied Mechanics and Materials Vol. 679 (2014) pp 254-260
© (2014) Trans Tech Publications, Switzerland
doi:10.4028/www.scientific.net/AMM.679.254

Submitted: 2014-08-13
Accepted: 2014-08-13
Online: 2014-10-08

Differentiation of Harmonic Current Effect at T- joint and Corner Joint on Three Phase 100kVA Transformer Losses

Dina Maizana [a] , Emi Zurima Bt Ismail [b], Nuriziani Hussin [c]

Department of Electrical System Engineering

Universiti Malaysia Perlis, Malaysia

E-mail: [a]dina@unimap.edu.my, [b]ezurima@gmail.com, [c]nuriziani@unimap.edu.my

Keywords: Harmonic current, T - joint, corner joint, transformer

Abstract. This paper describes the harmonic current effect at T- joint and corner joint on 3 phase 100kVA transformer model. The methodology that used to measure a harmonic current is using search coil connected to oscilloscope. The experiment is conducted by changing input voltage with different flux density. From the results obtained, the 3rd order harmonic current shows the highest for both T – joint and corner joint. The highest harmonic occurred at T – joint. For in plane, the harmonic current is 0.237A at corner joint and 0.389A at T - joint. At normal condition, the harmonic current were 0.250A and 0.769A at corner joint and T – joint respectively. This happened because of more energy required for transferring the flux to the left and right of the core. The corner joint of harmonic is less since the flux direction is 90° thus smaller amount of energy is required for the movement.

Introduction

Distribution transformer is a transformer that takes voltage from a primary distribution circuit and "step down" or reduces it to a secondary distribution circuit [1]. In the whole power system, the performance of transformer will give a high effect. They are a lot of cases can be explored from transformer. Even until now, many researchers have found new things regarding transformer. When refer to [2], the localized power loss of 100kVA 3phase distribution transformer has been investigate. The transformer lamination used was mix 60° - 45° in different layers of T – joints. The power loss at outer edge was higher than power loss at inner edge. The butt and lap joint was 18% less efficient than mitred joint. This is due to the rotational flux and the greater volume of saturated material used [3]. As refer to Fig. 1, fundamental frequency is 50Hz, when the frequency is added by multiple of three, the order of harmonic will become third order. Same if frequency added by multiple of five, the order of harmonic will become fifth order. It clearly stated that the sum of first harmonic until fifth harmonic will become a complex waveform. Positive sequence of harmonic will have similar phase rotation as fundamental voltage frequency, 50 Hz. The first, seventh, thirteenth and nineteenth order of harmonic are the example of positive sequence harmonics [4]. Efficient design of transformer core can be found from different cutting angle such as 23º, 45 º and 60º at the T-joint. To measured the localised flux density was using the search coil. The fundamental, third and fifth harmonic at the corner joint and T-joint in the normal and in-plane flux density form were measured [6, 7].

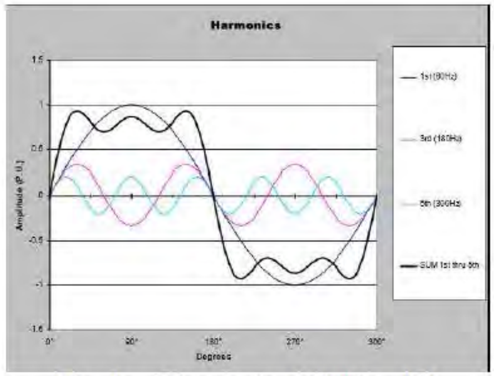

Fig. 1: Harmonic definition [5]

Fourier series can be used to show how a complex waveform is constructing. It is actually sum of all order of harmonic current occurred. The equation for harmonic content shows below:

$$Y = F_0 + F_1 \sin(\omega t + \varphi_1) + F_2 \sin(\omega t + \varphi_2) + \cdots + F_n \sin(\omega t + \varphi_n) \quad (1)$$

Hence, the reason of this investigation is to analyze the harmonic current at T – joint and corner joint on 100kVA transformer core lamination.

Experimental setup

The experiment was done by using three phase 100kVA transformer. This transformer consists of 254 turns for both primary and secondary winding. 3% SiFe Cold Rolled Grain Oriented, (CRGO) M5 is used as core lamination and total number of layer is 36. The core thickness is 0.3mm and 10cm as width. The overlapping of core lamination is 0.5cm length. A search coils were assembled at T – joint on 33^{rd} layer while for corner joint was on 36^{th} layer. Fig.2 shows the transformer core lamination.

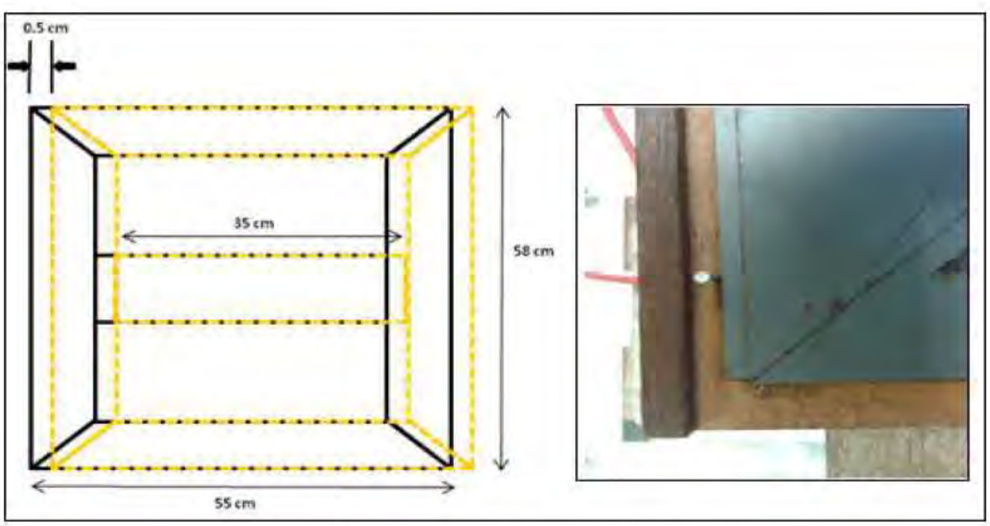

Fig. 2: Arrangement of the transformer core

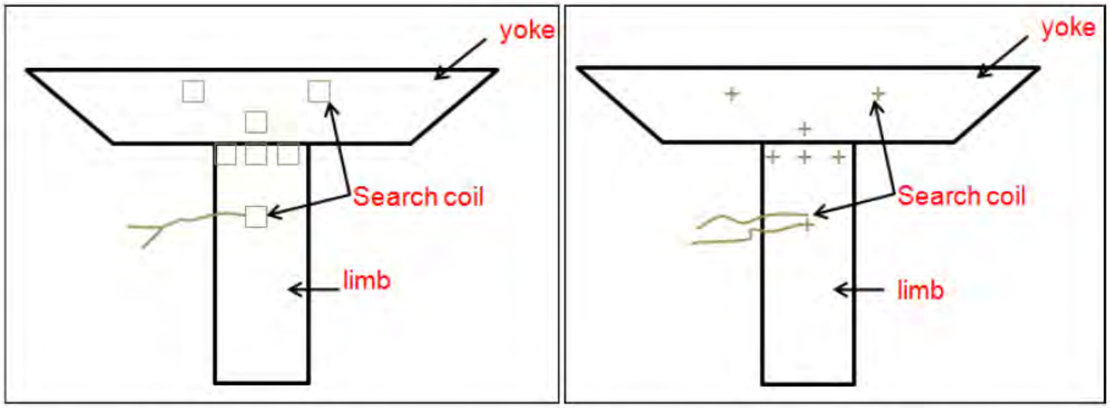

Fig. 3: The arrangement of search coil for normal and in-plane at T – joint.

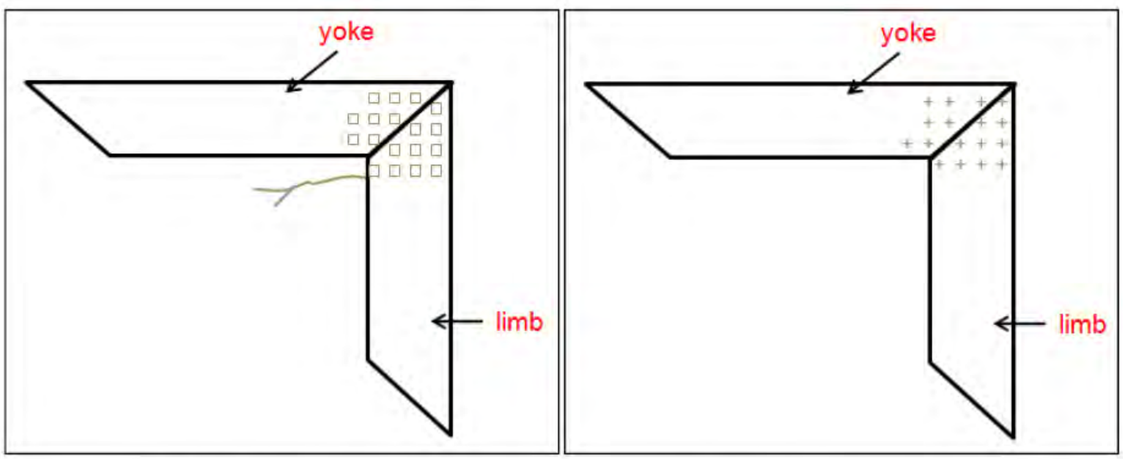

Fig. 4: The arrangement of search coil for normal and in plane at corner joint.

Fig.3 and Fig.4 show the arrangement of search coil for normal and in plane at T – joint and corner joint respectively. The search coil then was connected to oscilloscope in order to measure the harmonic value for every search coil. For arrangement of the equipment, the power analyzer that connected to the ac variable current gave an input current. The secondary side of transformer gave voltage to power analyzer. The experiment was conducted by changing the input voltage with different flux density. Fig. 5 shows the arrangement of the equipment. AC variable voltage as input was adjusted from 0.2T to 2.0T at 50 Hz. The equation used to get the input voltage is shows below:

$$V = 4.44 \times B \times N \times f \times A \quad (2)$$

Where:

V = Voltage, 4.44 = Constant, B = Flux density (Tesla), N = Number of winding turn = 254 turns, f = Frequency = 50 Hz

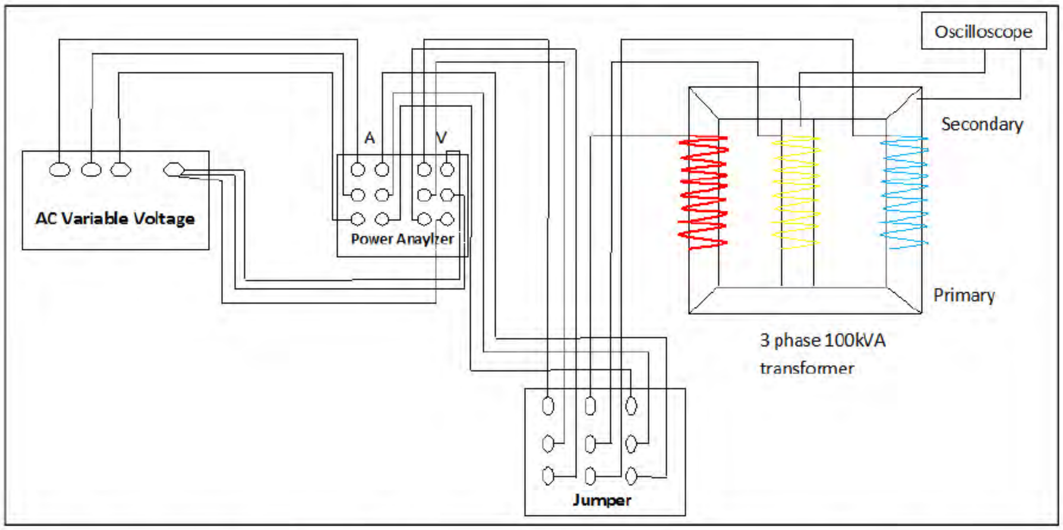

Fig. 5: The experiment setup for T – joint and corner joint measurement (single line diagram)

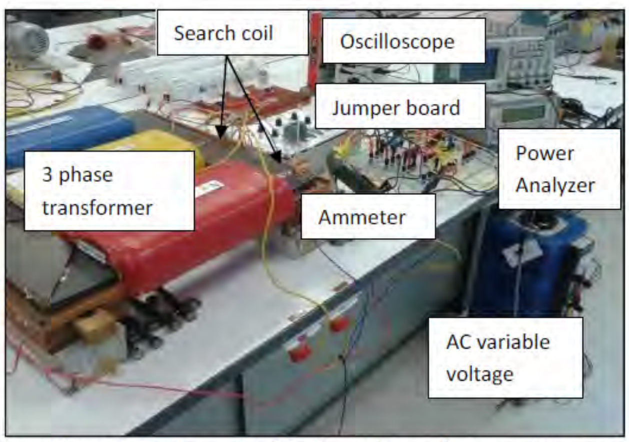

Fig. 6: The real experiment setup for T – joint and corner joint measurement

Fig.6 shows the real experiment setup for T – joint and corner joint measurement. Table 1 shows the calculation result from Equation 2 for input voltage from 0.2T until 2.0T at 50 Hz.

Table 1: Calculation result for input voltage

Flux density, B [Tesla]	**Input Voltage, V_{in} [Volt]**
0.2	11.97
0.4	23.93
0.6	35.90
0.8	47.86
1.0	59.83
1.2	71.80
1.4	83.76
1.6	95.73
1.8	107.70
2.0	119.66

Result & Discussion

After getting a data from the experiment, the value is transformed into a graph format using Matlab software. Fig. 7 and Fig. 8 show a waveform obtained from the experiment data at T – joint and corner joint respectively at 1.2 Tesla, 50 Hz. All of the harmonic waveforms are labelled for easy observation. The 3rd harmonic shows the highest compared to 5th and 7th harmonic for both position.

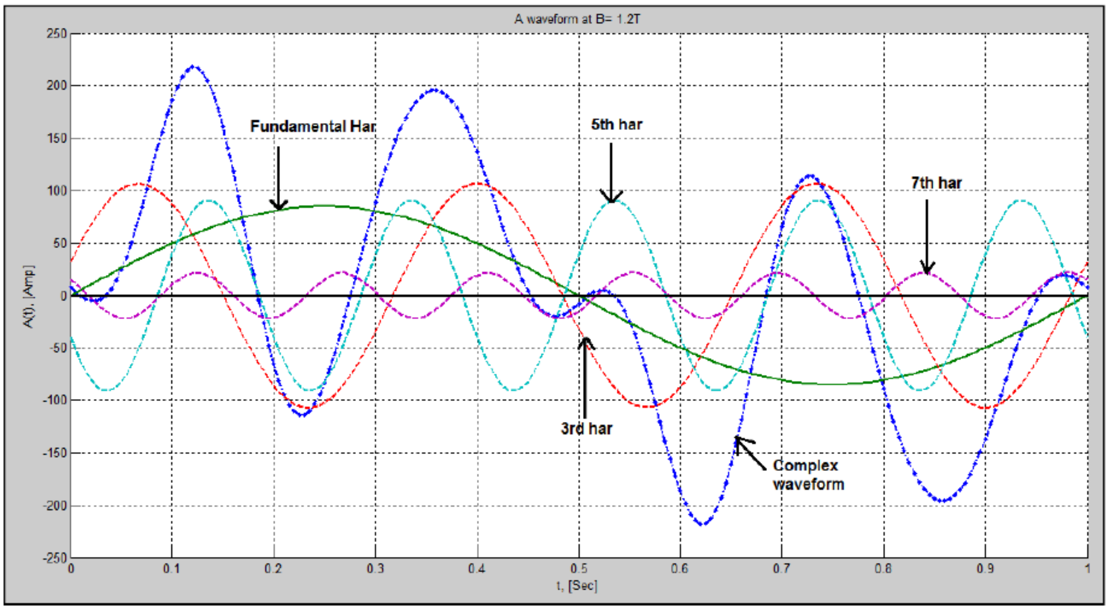

Fig. 7: A waveform for normal at corner joint at B=1.2T, 50Hz

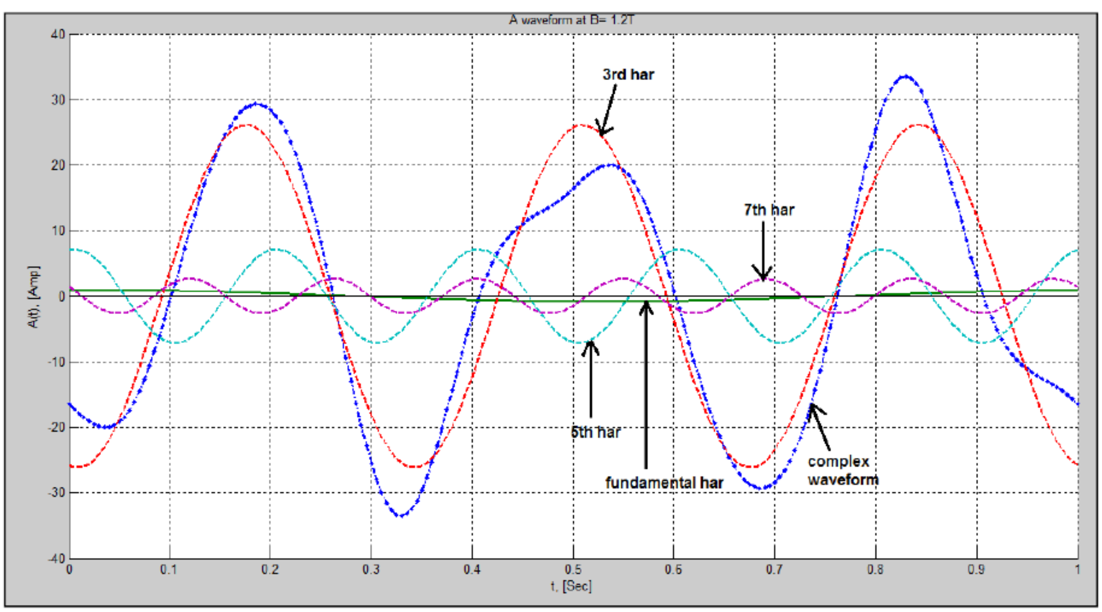

Fig. 8: A waveform for in-plane at T- joint at B=1.2T, 50Hz

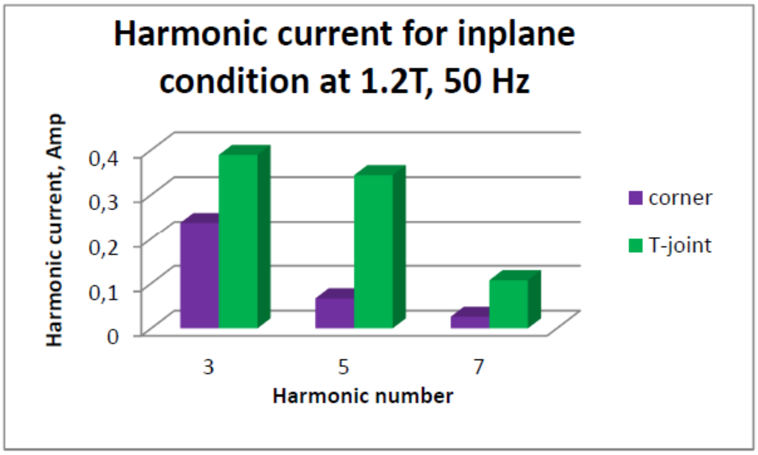

Fig.9: Harmonic current for in plane at 1.2T, 50 Hz

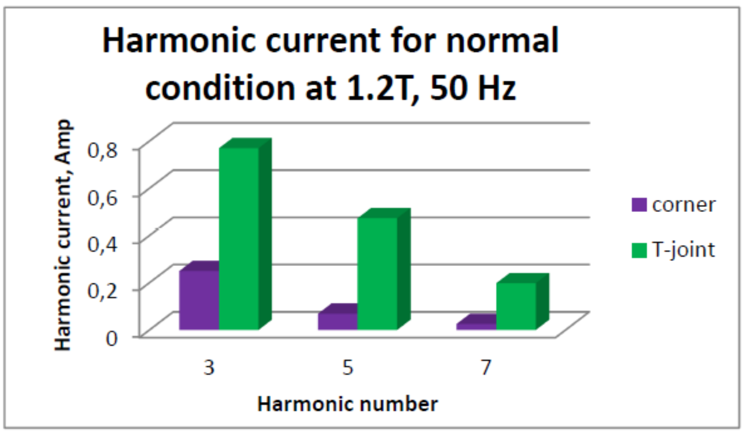

Fig.10: Harmonic current for normal at 1.2T, 50 Hz

Fig.9 shows the difference of harmonic current for in plane at 1.2T, 50Hz between T–joint and corner joint of transformer core. From the bar graph, the highest harmonic current occurred at 3rd order harmonic for both T – joint and corner joint while the lowest harmonic current occurred at 7th order harmonic. When compare the 3rd order harmonic current, T –joint was higher than corner joint which was 0.389A and 0.237A respectively. Fig.10 shows the difference of harmonic current for normal at 1.2T, 50 Hz between T –joint and corner joint of transformer core. The graph is similar to Fig.9 where the highest 3rd harmonic current occurred at T- joint. At corner joint and T- joint, the harmonic current were 0.250A and 0.769A respectively. These show that harmonic current occurred at T-joint was higher than at corner joint of the transformer core for normal and in-plane. This is because at T- joint, the change of flux direction happened where more energy required in order transferring the flux to the left and right direction of the core. The harmonic current less occurred at corner joint because the flux direction is at 90° thus smaller amount of energy required for the action.

Summary

From the overall investigation, the highest harmonic current was the 3rd order harmonic for T – joint and corner joint. The highest harmonic current appears at T- joint for both normal and in-plane. This happened because of more energy required for transferring the flux on different direction. The corner joint of harmonic is less since the flux needs a smaller amount of energy to transfer from one lamination to other lamination.

Acknowledgement

This work is financially supported by Grant RAGS FASA 1/2012 (9018-00025).

References

[1] Information on http://www.powerqualityinternational.com/resource-center/the-harnomic-problem/13-resource-center/110-harmonics-technical-overview

[2] D.M.M. Ahmad, 2010. Evaluation of the Localised Loss Transformer Core Lamination. *Journal of Applied Sciences, Vol. 10, Pg. 2917-2922*

[3] Mansel A. Jones and Anthony J. Moses, Comparison of the Localized Power Loss and Flux Distribution in the Butt and Lap and Mitred Overlap Corner Configurations, IEEE Transaction on Magnetics, Vol. Mag-10, No. 2, June 1974

[4] Ir. Dr. Mohamed Fuad Faisal, Managing Power System Harmonics, Asset Management Department Distribution Division TNB, 2012.

[5] Information on Michael Leporace,Harmonic Design Considerations, Specification Engineer, http://www.geindustrial.com/publibrary/checkout/Harmonic?TNR=White%20Papers|Harmonic|generic

[6] Shuhaimi, Zakaria@Abdullah, 'Flux density and power loss distribution in 100kVA Distribution Transformer core assembled with different cutting angle of T-joint', School of Electrical Systems Engineering (Theses), UniMAP ,2010

[7] Ismail Daut, Syafruddin Hasan, and Soib Taib, 'Magnetizing Current, Harmonic Content and Power Factor as the Indicators of Transformer Core Saturation', Journal of Clean Energy Technologies, Vol. 1, No. 4, October 2013

[8] K. Y. Yoon and S. S. Rao, 'Dynamic Load Analysis of Spur Gears Using a New Tooth Profile', *Journal of Mechanical Design*, Vol. 18, Issue 1, Pg. 1-6, December 2007

Engineering and Technology Research

10.4028/www.scientific.net/AMM.679

Differentiation of Harmonic Current Effect at T-Joint and Corner Joint on Three Phase 100kVA Transformer Losses

10.4028/www.scientific.net/AMM.679.254

5. https://www.scientific.net/AMM.679.247

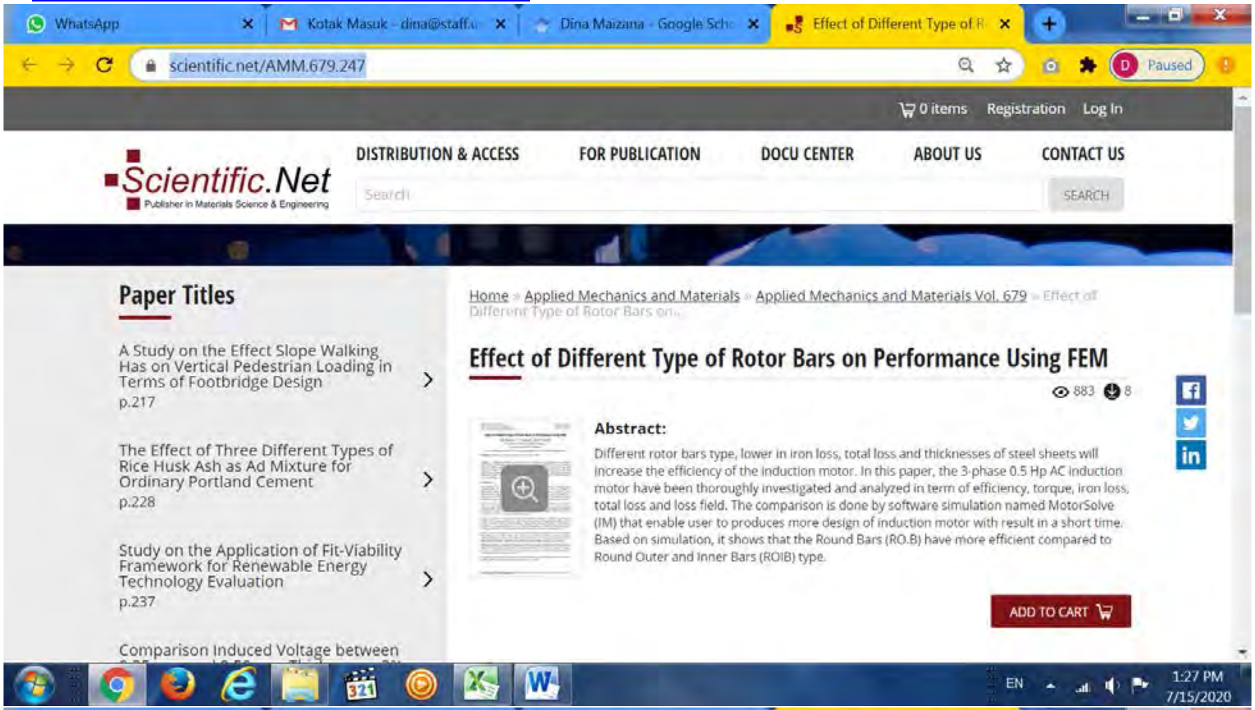

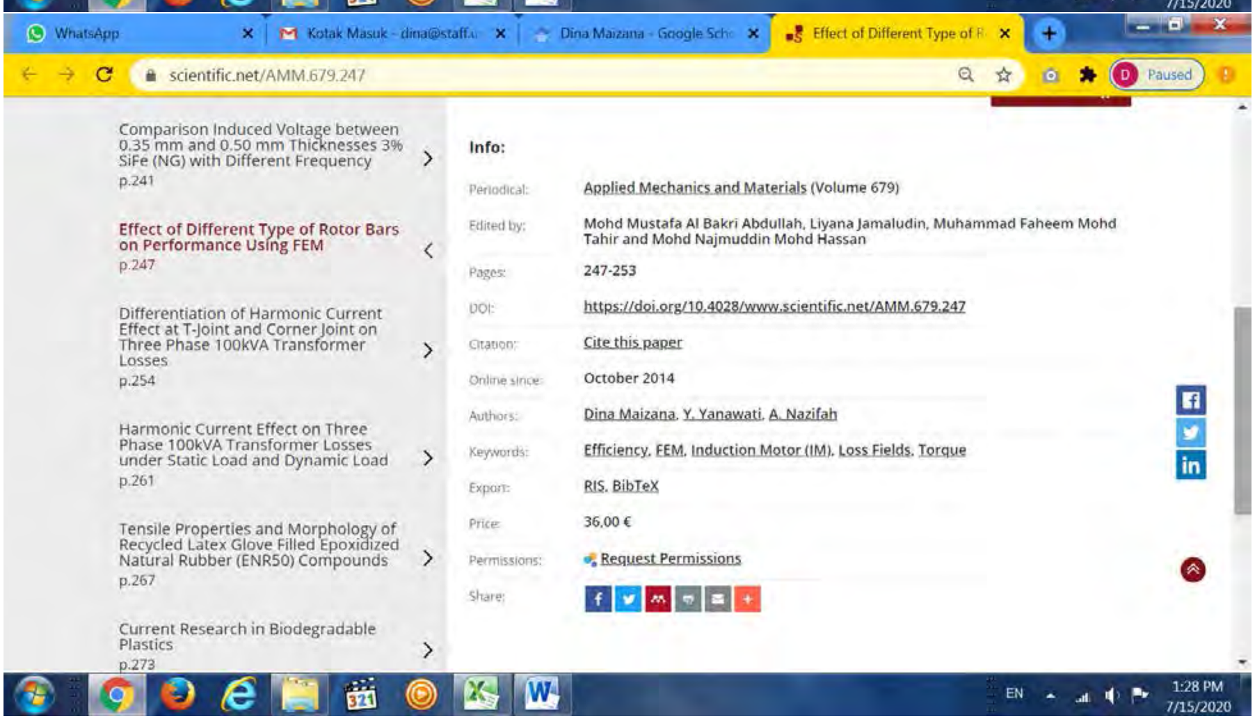

Applied Mechanics and Materials Vol. 679 (2014) pp 247-253
© (2014) Trans Tech Publications, Switzerland
doi:10.4028/www.scientific.net/AMM.679.247

Submitted: 2014-08-13
Accepted: 2014-08-13
Online: 2014-10-08

Effect of Different Type of Rotor Bars on Performance Using FEM

Dina Maizana[a], Y. Yanawati[b], and A. Nazifah[c]

Department of Electrical System Engineering

Universiti Malaysia Perlis, Malaysia

Email: [a]dina@unimap.edu.my, [b]yanawatiyahya@yahoo.com, and [c]nazifah45@gmail.com

Keywords – Efficiency, torque, loss fields, induction motor, FEM

Abstract – Different rotor bars type, lower in iron loss, total loss and thicknesses of steel sheets will increase the efficiency of the induction motor. In this paper, the 3-phase 0.5 Hp AC induction motor have been thoroughly investigated and analyzed in term of efficiency, torque, iron loss, total loss and loss field. The comparison is done by software simulation named MotorSolve (IM) that enable user to produces more design of induction motor with result in a short time. Based on simulation, it shows that the Round Bars (RO.B) have more efficient compared to Round Outer and Inner Bars (ROIB) type.

Introduction

In a significant horsepower size, three-phase induction motor drive a variety of industrial more equipment than any other way. Best of familiar three-phase induction motor are included in following key kind of NEMA (National Electrical Manufacturers Association) design B: normal torques, normal slip, normal locked amperes, NEMA design A: high torques, low slip, high locked amperes, NEMA design C: high torque, normal slip, normal locked amperes, NEMA design D: high locked-rotor torque, high slip and Wound-rotor: Characteristic depends on external resistances [1].

Industry sets out the several of speed and torque in demand for three-phase induction motor. 4 pole motors are most commonly, was followed by 2 poles, then 6 pole motor. There are plenty of distinct torque demands, from zero to full load speed. Of several loads need a very high starting torque. Another load requires bit starting torque; however the torque demand higher speed increases. The design letter helps in choosing the right/correct motor [2].

There are two kinds of rotor induction motor can be placed in the stator which are cage rotor and wound rotor. A cage induction motor rotor consists of a series of conducting bars laid into slots carved in the face of the rotor and shorted at either end by large shorting rings. This design is referred to as a cage induction motor rotor because the conductors. Wound-rotor induction motors are more expensive than cage induction motors and they require much more maintenance [3].

However, motor manufacturers will no longer be able to offer standard-efficiency motors in 1997. The Energy Act of 1992 defines and proposes new efficiency levels for several electrical component including motors. It is assumed that as motors wear out, replacement motors will be the high-efficiency offerings. High-efficiency motors are built to reduce energy loss in motor [4].

The eddy currents are restrained by lamination. If the core metal is subdivided into thin sheets the balance of eddy current path resistance and induced emf shifts so that the overall power wastage in the core is radically reduced. The thinner the steel sheet the more effectively eddy currents are restrained and the lower the core losses [5].

In this paper, the performance comparison on Round Bars (RO.B) and Round Outer and Inner Bars (ROIB) with 0.35 mm thickness for Induction Motor is presented.

MotorSolve (IM) Software

MotorSolve (IM) software is the design and analysis software that's right for induction motors and generators for automatic finite element results module. The easy to use template-based interface, including are dozens editable the rotor and stator type. Automatic coil winding characteristics ensure all optimal balanced layouts available for the current design. Figure 1 shows the MotorSolve (IM) Software workflow. Based on Figure 1, MotorSolve (IM) software was used to design the machine and take into account essential effects like Leakage Inductances, Iron Losses, Efficiency, Deep Bar Effects, Stator End Effects, Skewing and Effects of switching on motor characteristics due to inverter fed phases.

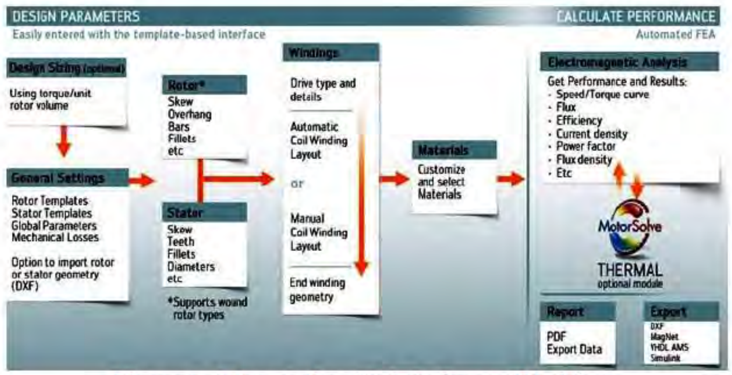

Figure 1: MotorSolve (IM) Software Workflow

MOTOR DESIGN BY FEM MODELING

The induction motor with two rotor bars types which are Round Bars (RO.B) and Round Outer and Inner Bars (ROIB) and parallel round stator was chosen for this simulation. Figure 2 (a) and (b) shows the design with two type of rotor bar with same stator slot type. Based on Figure 2 (a) Round Bars Rotor Type and Parallel Round Stator Type and (b) Round Outer and Inner Bars Rotor Type and Parallel Round Stator Type, the model of the induction motor is 3-phase, 0.5 Hp, 420 V, 50 Hz with 30 rotor bars of Round Bars (RO.B) and Round Outer and Inner Bars (ROIB) rotor type and 24 stator slots of Parallel Round teeth. Only the rotor bar type was changed with same thickness for rotor frame for each simulation.

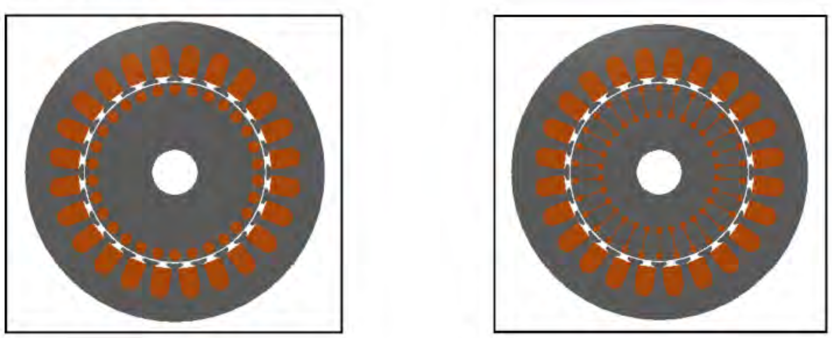

(a) (b)

Figure 2: Two Types of Rotor Bars with Same Stator Slot Type

Figure 3 shows the FEM software simulation by using the AC Analysis solver. The result is then compiled to Table 1 which is the nameplate data of 0.5 Hp induction motor for Round Bars (RO.B) and Round Outer and Inner Bars (ROIB) with 0.35 mm thickness non-oriented steel sheets. The input like motor horse power, input voltage and frequency are included in FEM software and the remaining result in Table 1 are output from the FEM software simulation.

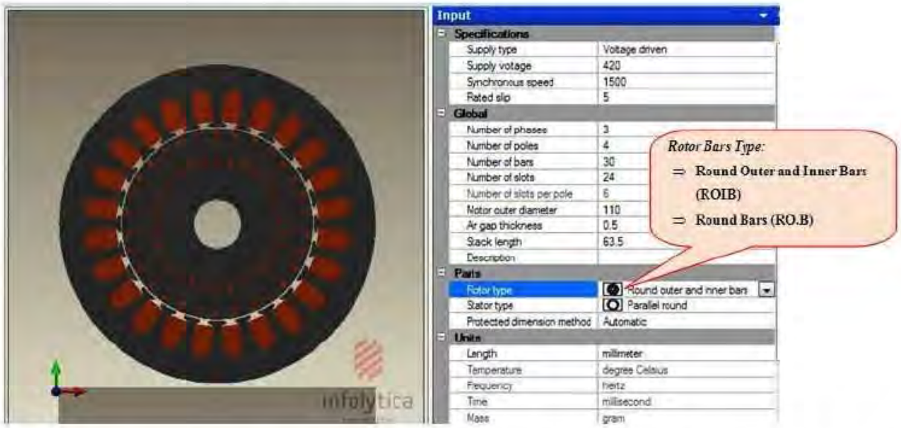

Figure 3: The Designed FEM model with 2 Types of Rotor Bars for 3-Phase 0.5 HP Induction Motor

Table 1: 3-Phase 0.5 Hp induction motor nameplates for 2 Types of Rotor Bars

Round Bars (RO.B)		Round Outer and Inner Bars (ROIB)	
Phase	3	**Phase**	3
Frequency	50	**Frequency**	50
Voltage	420	**Voltage**	420
RPM	1425	**RPM**	1425
Current	1.1746	**Current**	1.1664
Horsepower	0.5	**Horsepower**	0.5
Power Factor	0.6216	**Power Factor**	0.5826
Efficiency	76.92	**Efficiency**	76.02

Figure 4 (a) and (b) shows the design specification of the induction motor in millimeters for both rotor bars type with same thicknesses (0.35 mm). Based on Figure 4 (a) and (b), it shows the Round Bars (RO.B) and Round Outer and Inner Bars (ROIB). Use of these slot design is due it has a 'started bar' discretely separated from the main body of the conductor bar by 'slot leakage', related to the motor with the high conductivity material in the rotor cage. In addition, these designs have a rotor bar higher torque locked rotor and high slip [6].

(a) Round Bars (RO.B) (b) Round Outer and Inner Bars (ROIB)

Figure 4: Design for 2 type of Rotor Bar

Analysis Result and Discussion

Induction motor design were analyzed using analysis and performance charts for the features like efficiency, torque, iron loss, total loss, and eddy current loss.

Figure 5 shows the efficiency vs. Speed for two (2) type of Rotor Bar which are Round Bars (RO.B) and Round Outer and Inner Bars (ROIB). Based on Figure 5, the graph shows that the value of efficiency at 1425 rpm for Round Bars (RO.B) is higher than Round Outer and Inner Bars (ROIB), which are 76.92% and 76.02% each. The Round Bars (RO.B) has an increment of 1.2% for the efficiency as compared to Round Outer and Inner Bars (ROIB). It is because when efficiency increases, the losses in induction motor will be decrease.

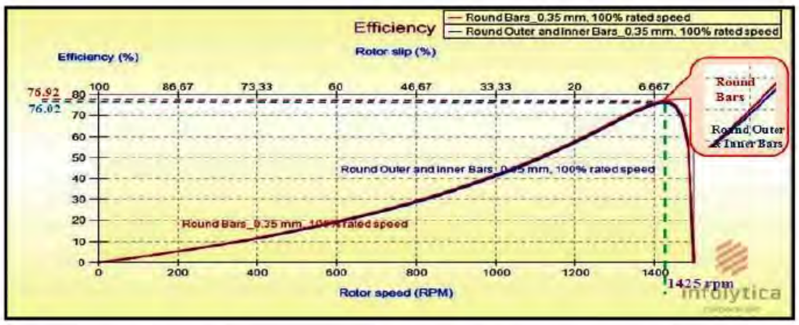

Figure 5: Graph Efficiency vs. Speed for Two (2) type of Rotor Bar

Figure 6 shows the Two (2) type of Rotor Bar. According simulation, refer to Figure 6, when speed at 0 rpm it showed that the Round Bars (RO.B) is higher starting torque than the Round Outer and Inner Bars (ROIB) type which are 6.27 Nm and 4.24 Nm each. It shows that Round Bars (RO.B) is better than Round Outer and Inner Bars (ROIB) type. This is because for the Round Bars (RO.B), at a faster speed fractional, the heat produced from the motor is less, the terms of the rotor core is commonly associated with loss or core loss can be minimized and can even render damage to the motor at a minimum compared to Round Outer and Inner Bars (ROIB) type.

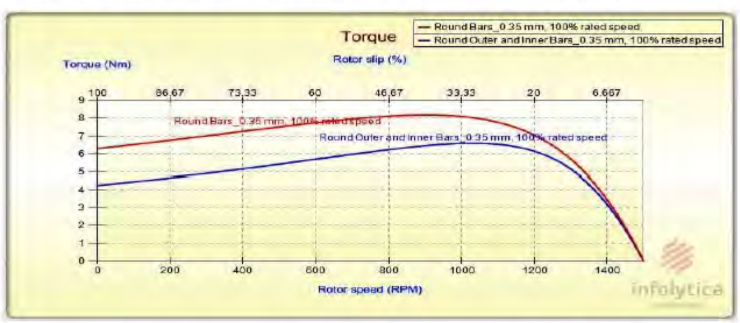

Figure 6: Torque vs. Speed for Two (2) type of Rotor Bar

Iron losses happen in all sections of iron as the magnetic field different machine. An iron loss has two components, hysteresis and eddy current losses which is happen in other parts of iron depends on the frequency of requested voltage. Figure 7 shows the graph of Iron Loss vs. Speed for Two (2) type of Rotor Bar. According to the Figure, at 1425 rpm, the value of iron losses for Round Bars (RO.B) and Round Outer and Inner Bars (ROIB) are 4.0691 Watt and 4.1077 Watt. The Round Bars (RO.B) decreased of 0.94% for iron loss compared to the Round Outer and Inner Bars (ROIB) type. It is because; decrement of lamination steel sheet, size and number of rotor bars can reduce the iron loss

Figure 7: Iron Loss vs. Speed for Two (2) type of Rotor Bar

When the speed reached at 1425 rpm (highlighted) the total losses for Round Bars (RO.B) type are 118.55 Watt where else for Round Outer and Inner Bars (ROIB) it is 121.35 Watt as shown as Figure 8. This shows that the power loss for Round Bars (RO.B) is lower than the Round Outer and Inner Bars (ROIB) type. The Round Bars (RO.B) decreased of 2.31% for total loss compared to the Round Outer and Inner Bars (ROIB) type. This is because Round Bars (RO.B) type has lower resistivity and lower the heat generated compared to the Round Outer and Inner Bars (ROIB) at that rpm.

Figure 8: Total Loss vs. Speed for Two (2) type of Rotor Bar

Figure 9 (a) and (b) shows the comparison of Hysteresis-Lamination Eddy Current Loss for Two (2) type of Rotor Bar which are Round Bars (RO.B) and Round Outer and Inner Bars (ROIB).

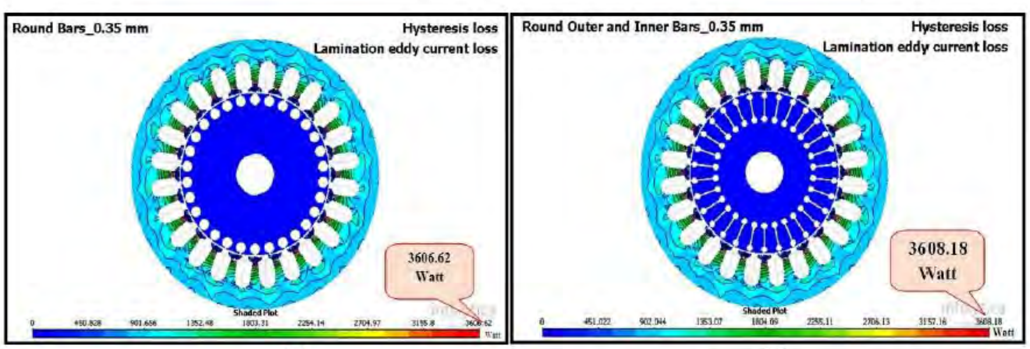

(a) (b)

Figure 9: Hysteresis-Lamination Eddy Current Loss for Two (2) type of Rotor Bar

Refer to Figure 9 (a) and (b), it shows the comparison between Two (2) type of Rotor Bar in terms of eddy current loss. Both of the Figure shows that the lamination eddy current loss for Round Bars (RO.B) has lower than Round Outer and Inner Bars (ROIB) type. The values of lamination eddy current loss for both rotor bars type are 3606.62 Watt and 3608.18 Watt each. The Round Bars (RO.B) shows 0.04% lower lamination eddy current loss compared to Round Outer and Inner Bars (ROIB) type. The lamination eddy current loss can reduces with decreasing thickness of rotor frame. The magnetic core loss can also be reduced by using thinner lamination in the magnetic structure.

MotorSolve (IM) software is capable to produce flux and current density has shown as Figure 10 (a) and (b). Based on that Figure, the Contour plot field (Contour lines) will produce the Flux in Phase, while the Shaded plot field (colour) represents the Current density.

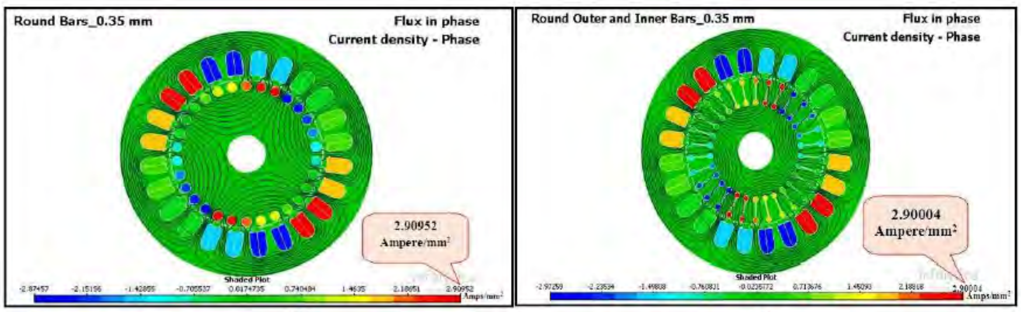

(a) (b)

Figure 10: Flux-Current Density for Two (2) type of Rotor Bar

Based on Figure 10 (a) and (b), it shows the Current Density for Round Bars (RO.B) has higher than Round Outer and Inner Bars (ROIB) type. The values of current density for Two (2) type of Rotor Bar are 2.90952 Ampere/mm^2 and 2.90004 Ampere/mm^2 each. The Round Bars (RO.B) shows 0.33% higher current density compared Round Outer and Inner Bars (ROIB) type. The total current is higher when the current flow into a smaller rotor bars. It can caused the amount of torque will be higher than the bigger rotor bars. The value of current and flux density will be change due to the rotor bars size, thinner and losses.

Conclusion

From the analysis, it shows that the Round Bars (RO.B) has an increase of 1.2% for the efficiency, higher starting torque, a decrease of 0.94% for iron loss, a decrease of 2.31% for total loss, a decrease of 0.04% lamination eddy current loss and higher of 0.055% for current density as compared to that of Round Outer and Inner Bars (ROIB) type. High efficiency in induction motor can reduce harmonic and motor energy losses. Decrement lamination of steel sheet can reduce the eddy current loss. The value of current and flux density will be change due to the rotor bars size and types, thinner and losses.

Acknowledgment

This work is financially supported by Grant RAGS FASA 1/2012 (9018-00022).

References

[1] Ali Emadi (2005). Energy-Efficient Electric Motors (Third ed.): Marcel Dekker, Inc.

[2] Augie Hand (2002). Electric Motor Maintenance and Troubleshooting: McGraw Hill.

[3] Bottauscio, O., Chiampi, M., Concari, C., Tassoni, C., & Zucca, M. (2008). From the ideal to the real induction machine: Modelling approach and experimental validation. Journal of Magnetism and Magnetic Materials, 320(20), e901-e906.

[4] PT Design (1997). Motors, Power transmission design, vol. A340.

[5] Beckley P. (2002). Electrical Steels for rotating machines: IEE power and energy series; no.37.

[6] I. Daut, Y. Yanawati, N. Gomesh, S. Nor Shafiqin, M. Abdullah, I. Pungut (2010). "*Comparison of Torque between Different Diameters of Copper Rotor bar slot by Using FEM Software.*" 2010 3rd International Conference on Computer and Electrical Engineering (ICCEE 2010), 16-18 November 2010, Chengdu, China.

Engineering and Technology Research

10.4028/www.scientific.net/AMM.679

Effect of Different Type of Rotor Bars on Performance Using FEM

10.4028/www.scientific.net/AMM.679.247